THE PENNSYLVANIA STATE UNIVERSITY

DEPARTMENT OF ENGINEERING SCIENCE AND MECHANICS

EFFECT OF FLUID FORCES ON KINESIN AND MICROTUBLES IN GLIDING ASSAYS

SOUFIEH HAKIMZADEH-HOSSEINI

SPRING 2018

A thesis
submitted in partial fulfillment
of the requirements
for a baccalaureate degree
in Engineering Science
with honors in Engineering Science

Reviewed and approved by the following:

William Hancock
Professor of Biomedical Engineering
Thesis Supervisor

Gary Gray
Associate Professor of Engineering Mechanics
Engineering Science Advisor

Judith A. Todd
Department Head
P.B. Breneman Chair and Professor of
Engineering Science and Mechanics

Abstract

Microtubules are tubular structures within the cytoplasm of cells that are responsible for cell movements including intracellular transport and organelle movement. They play a large role in positioning cell parts for separation during mitosis and are also responsible for the movements of cilia and flagella. The motor proteins responsible for facilitating the movements in which the microtubules participate are labeled as kinesins and dynein [7]. The main difference between these motor proteins is that the kinesins travel along the microtubule toward the plus and the dynein travel toward the minus end. In this paper, we will be focusing primarily on kinesin, more specifically dmKin1 found in drosophila melanogaster (fruit flies). Motor proteins such as kinesin move their cargo (vesicles or organelles) along microtubules, which act as tracks within the cell that allows for the trafficking of all intracellular contents [25]. Kinesin contains a residue motor domain of two chains that uses ATP hydrolysis to move along the microtubule.

In this work, kinesin and microtubules were examined in order to understand their characteristics and to develop a screening method for further experimentation. Understanding kinesin characteristics could lead to more efficient ways of testing and ultimately help understand the role motor proteins play in the human body and diseases they are linked to. To do this, samples of dmKin1 kinesin and microtubules were prepared and passed through a gliding assay. When the microtubules are set in place, a solution is run over the top of them at various speeds and their reactions are recoded. The recoded data at different speeds show various microtubule movements or detachments and can demonstrate the effect of mechanical forces on these biologics. Three videos were selected at a high speed (20,000 nL/sec), speed (16,000 nL/sec) and a slower speed (8,000 nL/sec). These videos are further analyzed for any potential

trends or patterns. The purpose of this research is to observe motor cooperativity and force sensitivity. From this, a screening method was identified to distinguish characteristics of kinesin and determine if more in depth testing must be done with another characterization tool such as optical trapping.

Table of Contents

Table of Figures

Acknowledgements

Over the course of my four years at Penn State, I owe many thanks to those who have supported me and put in the effort to help me excel and succeed, most notably my parents and brother, my strong support network of friends and faculty in the Department of Engineering Science and Mechanics and Mechanical Engineering Department, and all my advisors and professors throughout the College of Engineering. I would like to specifically thank my Engineering Science advisors, Dr. Gary Gray and Dr. Lucas Passmore, for helping me manage my tight schedule of classes and always pushing me and believing in me. Dr. Gray's dedication to helping me manage an ambitious schedule pushed me to work as hard as I can. Had it not been for him, I would not have achieved as much as I did. Another thank you goes out to a member of the Hancock Lab Joseph Cleary, who would meet and guide me throughout this entire venture for two years. Without him I would still be stuck on how to download FIESTA onto my computer. A special thanks to my other thesis advisor, Dr. William Hancock, for allowing me to use his lab and resources and assisting me in choosing my thesis topic.

1. Introduction

Microtubules and kinesin motor proteins play major roles in cell viability, intracellular transport, and signaling. Without these components, vesicles and other cell organelles would rely on diffusion to move within the cell. These components are also significant in cell division (mitosis), which is essential for growth of tissues and organs, and are required for neuronal growth and survival. There are many types of kinesin, each with different characteristics, serving a different purpose or specific to a certain part of the body. For instance, kinesin-1 (the kinesin used in this study) is specific to transporting vesicles throughout the axon to assist in synaptic transmission. Kinesin-2 is known for intraflagellar transport and is what creates and maintains the flagella and cilia. And Kinesin 14 and 5 are known for assisting in mitosis and meiosis. Different kinesin move in different ways, some moving directionally, others using a head over head or power stroke method to move. Kinesin-1 is a highly processive motor that takes over a hundred steps for each motor binding. This motor moves along a microtubule in a "hand over hand" mechanism as shown in figure 1.1. This is the motor that is being studied and focused on within this research [7].
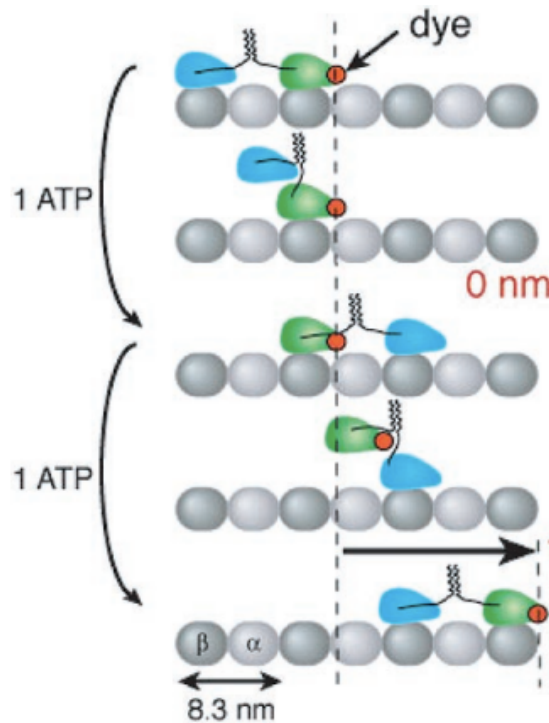
Figure1.1: Hand over hand method used by kinesin-1 to move cargo to the edge of the cell [33]

Up until now, the research that has been done has focused on kinesin or microtubules on their own. It is known that the single motor forces are between 6-8 pN. This is enough to overcome drag when moving small organelles such as vesicles, but results in complexity with larger cargos or within different cells. With larger cargos and more complex cells such as axons, which have more filaments and tighter geometries, kinesin motors need more force to pull. In a paper by Juliana C. Wortman, the argument is presented and explored that near the axon walls, drag increases enough to impede cargo transport, but having parallel microtubules close enough together, a cargo can engage in motors in summation from both microtubules that allow it to work cooperatively to enhance motor activity and minimize opposition to transport [32]. This poses the question of whether kinesin can work together to generate higher forces.

This research focuses on the interaction between the two for motor cooperativity and force sensitivity, effected by drag force. Previous studies done by labs such as the Diehl and

Furuta labs demonstrated that kinesin cannot work cooperatively. The Diehl lab suggested that kinetic barriers, such as the fact that it takes too long to create a two-kinesin complex to develop load-sharing configurations, restrict the cooperativity of kinesin [18]. The Furuta Lab showed how kinesin-14 productivity increased with cooperativity but kinesin-1 productivity increased minimally with cooperativity, showing that cooperativity relies the speed of microtubule binding kinetics and the drag force [9]. At the same time, there are many studies that demonstrate that motor cooperativity works well and motor proteins are able to sum forces well. At the same time, there is a lot of experimental evidence showing that motor cooperativity does sum the forces of kinesin well. For example, the Mallik lab has suggested that while strong kinesin tend to not work collectively, detachment prone dynein motors are able to generate higher forces with increased dynein number [24]. This demonstrates the difference between the motor proteins and how we do not fully understand them yet, which is the greater goal of this work. Analyzing the relationship between drag force and microtubule movement as well as kinesin properties such as detachment rates will identify patterns that could give new insight into cell behaviors. Specifically, force sensitivity can be observed through a concept known as stall force.

Stall force is when the force of the kinesin moving along the microtubule and the fluid force around it are equal, causing it to stall at its location and be unable to move anymore. Kinesin-1 was found to move slower in viscous fluids but also stall around a force of 6-8 pN which was found by placing an external force on the kinesin [28]. In this experiment, the external force was recreated with a volume flow rate creating a fluid force pushing against it. One popular way to track stall forces is a concept known as optical trapping [29]. There are two approaches to testing motor cooperativity optical trapping. In the first process, a bead is attached to a microtubule and light is used as an optical tweezer, where this attachment now identifies the

force that the microtubule is removed from (similar to a spring constant) [2]. A test similar to a creep test is performed on the microtubule and optical tweezer setting to determine its lifetime. In this setting, the force that it takes to remove the microtubule from the kinesin (similar to a spring force) is identifiable. The effectiveness and ability to fine tune the optical trap is based on laser power and intensity and how well the point spread function is assembled (the three-dimensional diffraction pattern of light).

The second method is similar to a tensometry test, where the microtubule and kinesin are interacting, but the optical tweezers are pulling them in a manner similar to a creep test. This is done until the microtubule pops off to observe a characteristic similar to the "ultimate tensile strength" of the kinesin. Another approach is to move the tweezers while keeping the stage stationary or to move the stage while keeping the tweezers stationary [8]. This allows the lifetime to be seen when the microtubule pops off its attached location. While optical trapping is good for specific quantitative data for one sample or one individual molecule, there are many factors that must be overcome with using this method. Because it is so specific and such a complex system, it takes a long time for each experiment to be performed. Using this method also takes a highly trained expert physicist as well as an expert on laser microscopy. The test would also require a high throughput test so that better statistical properties are obtained. Because of all of these factors, it is very difficult to perform experiments on kinesin and microtubules to determine their characteristics [27]. In this study, members of the Hancock Lab have come together to determine a new and more efficient method of determining kinesin lifetime and kinesin characteristics through experimentation, simulation, and matlab analysis.

This research is most specifically focused on full length kinesin 1. Kinesin and dynein are two families of motor proteins, but the difference between them is the type of cargo they carry

and the direction of movement (kinesin moves cargo toward the periphery of the cell while dynein carries it to the center of the cell). Full length kinesin 1 was identified in 1985 based on its movement in the cytoplasm of an axon of a squid. This discovery was led by researcher Ron Vale and colleagues who created an assay for real time observation of transport *in vitro* . For a long time, kinesin-1 was the only known motor protein that moved towards the plus end of a microtubule but during the 1990s, many other kinesin proteins were reported. Kinesin 1 is commonly referred to as conventional kinesin, kinesin heavy chain or KHC, and is a motor protein that utilizes chemical energy from ATP hydrolysis to create mechanical force [16]. Kinesin 1 is part of a greater superfamily known as 1bg2A which classifies all the motor proteins [10]. Full length kinesin 1 is the full motor protein that contains two motor heads and two small globular tails while a truncated kinesin is fragmented. The full-length kinesin is used in order to accurately represent how fluid forces would interact in the body. It is important to keep in mind that this research is not focusing on any particular illness, but instead we are looking at the underlying physiological reasons for why these illnesses could be occurring. By understanding how kinesin and microtubules act and are affected by mechanical forces, it is hoped that a baseline could be developed for models of illnesses in vitro. This means that improvements can be made in healthcare, and in-patient safety. For instance, diseases such as frontotemporal dementia, ALS, and deafness have been linked to kinesin motor dysfunctions in a paper by Eckhard and Eva- Maria Mandelkow [20] .

If more information could be found about the biophysical properties and how these biological systems react to external sources, new steps could be taken towards preventing, treating, and curing these illnesses. Economically, if this research could lead to more efficient and cheaper medication or even cures, it would be much more economical for the patient than to

pay for constant treatment and inefficient care. It could also lead to personalized medicine which would have a higher efficiency and reduce the money spent on multiple medications at once. Better understanding of the characteristics of kinesin and microtubules could also lead to better understanding of how organelles are moved within plant cells, which could ultimately lead to increased crop yields, more environmentally responsible agriculture, and plant-based pharmaceutical production.

1.1. Project Statement

The goal of this project was to investigate the behavior of (K980) full length dmKin1: drosophila melanogaster kinesin and microtubules under mechanical forces, specifically drag force in a gliding assay. This was done to create a screening method to determine if a motor protein is stochastic or cooperative. This screening method could work for any motor; kinesin, dynein, or myosin. The screening method would determine if the more in-depth characterization needs to be done to understand the motor protein. For example, if a motor is determined to be cooperative, it would be clear that the next step would be to perform optical trapping to understand what is happening in the kinesin interactions. The process of using this screening process would be do obtain the motor, perform a gliding assay test on it, run through the analysis/screening method performed in this study, and then determine if further experimentation such as an optical trap would be necessary. Software such as ImageJ and FIESTA was used to assist in the calculations and modeling of the video results. FIESTA stands for florescence image evaluation software for tracking and analysis and is used to obtain a set of parameters from the video of moving microtubules within the plane. These parameters include frame number, time, x coordinate, y coordinate, z coordinate, distance, length, amplitude, orientation, and tags. Captured videos were then analyzed in FIESTA and

data was run through matlab code to sort information into visuals. Various matlab scripts were written to sort through the data based on the sorting categories. The sorting categories included perpendicular and parallel forces, velocity, and angle. The codes written sort and graph the data from FIESTA into Force vs Velocity graphs and Angle vs. Velocity graphs for parallel and perpendicular flow, as well as Force vs Length. The radius of curvature was also found for all the paths in all three examined flow velocities. The "force" being discussed throughout this study is the drag force as defined previously.

2. Theory

2.1. Motor Cooperativity and Stochasticity

Motor cooperativity is when more than one motor protein such as kinesin work together to serve a function. Motor cooperativity is critical in transport kinesin (kinesin 1, 2, 3) because it is paramount to mechanisms that coordinate and balance the internal organization of eukaryotic cells. Motor proteins such as kinesin 1,2, or 3 often work together to move organelles or vesicles throughout the cell. The combined power of all the motor proteins working on a particular cargo determines if it could be transported over longer distances or if it can move against higher opposing forces. The more kinesin attached to a cargo, the stronger the bond, the longer the distances, and the stronger opposing forces it can move through [5].

Motor cooperativity is also seen in the intraflageller transport chain (IFT). The IFT is seen in motor organelles such as cilia and flagella, which are projection from the cell that allow it to move. Defects in the IFT have been shown to result in some human diseases due to the fact that cells are no longer mobile in the human body [26]. The main purpose of cilia in eukaryotic cells is to move fluid or cells over the surface of the extracellular fluid. IFT is what moves non-membrane bound particles from the cell body throughout the cilia or flagella and then back to the cell body [3]. IFT is critical because it contributes to cell motility and cilium based signaling. The image below shows how the motor proteins kinesin II and dynein move along the microtubules within the IFT.

Nature Reviews | Molecular Cell Biology
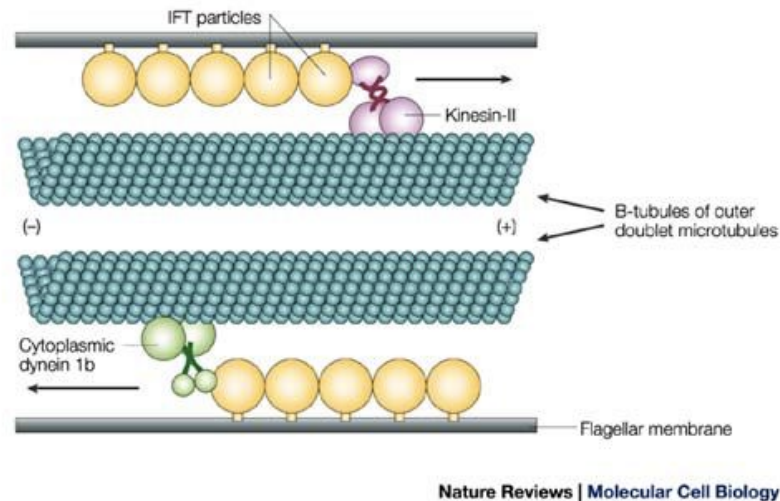
Figure 2.1: Model of motor protein interaction and microtubule within IFT [17]

Forward and backward IFT are led by two members from the kinesin-2 group that work to ensure the motor organelles are working properly. Kinesin-II motors mediate cargo forward from the cell body to the end of the cilia and flagella. From there, another motor protein (dynein 1B) moves the particles back to the cell body [13].

Although this study does not focus on this motor protein, myosin also utilizes the concept of motor cooperativity. Myosin is another form of motor protein. While kinesin and dynein move along tubulin filaments, myosin moves along actin filaments and coupled hydrolysis of ATP (adenosine tri phosphate) to create energy to move the motor protein [15]. Myosin move along actin filaments as their head contains a lever that acts as a mounting device. Each actin filament is attached by multiple myosin heads that work together to move the actin along. This movement is known as a power step and is best illustrated in an image.
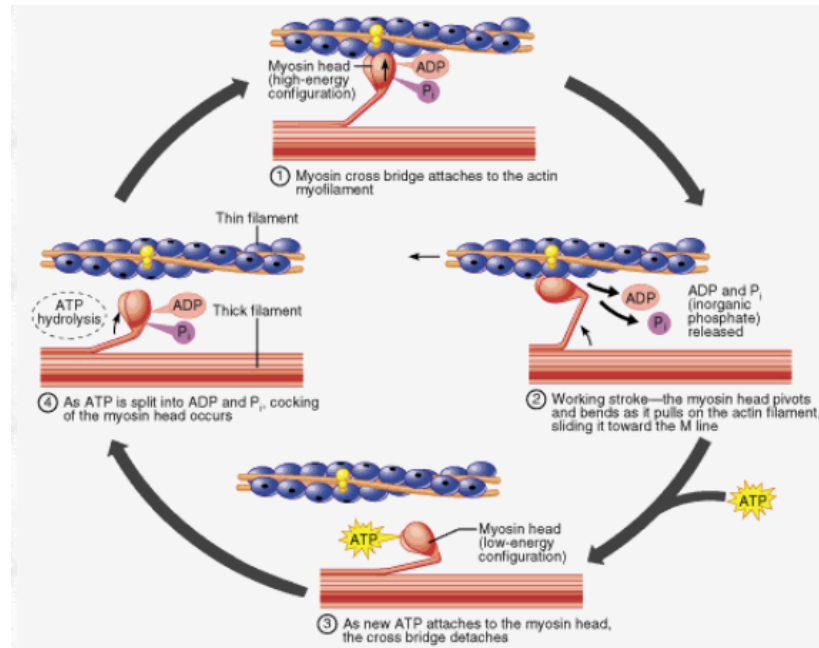
Figure 2.2: Diagram of the power step within a muscle contraction [22]

The mechanical work that the movement of the mounting device entails directly impacts the rate of ATP usage [30]. Myosin are commonly found in muscle tissue, and with each muscle contraction, cooperativity of myosin is required to move molecules within a thick actin filament.

Stochasticity is when all the kinesin bonded to a microtubule do not work at a team, and work independently of each other [31]. This means that if a force was acting on the microtubule –kinesin system, and one kinesin bind broke, the remainder of the kinesin would still be bonded because they are all independent motors [23]. As opposed to a cooperative system where if one kinesin binds broke, the entire system would detach.

2.2. Force Sensitivity

It is known that each type of kinesin has a different force sensitivity. For instance, kinesin 1 is the most recognized kinesin and has a stall force of about 6-8 piconewtons [29]. After that, kinesin 2 has a such a small stall force that it is unidentifiable and the stall force for

kinesin 3 is even less than that. Each kinesin can carry a cargo that is up to 400 times the size

of the kinesin, yet they are still able to move it and support it. This is because on each cargo

is not a singular kinesin, but a team of kinesin participating in multi motor kinesin interaction

to help carry this load to its destination [18]. Force sensitivity is also a factor in

understanding if a kinesin is cooperative or stochastic.

2.3.   Drag Force

Drag force is a mechanical force created by the interaction between a solid body with

a fluid when there is motion between the solid and the fluid [12]. In this case the solid is the

microtubule and the fluid is the solution being passed around it within the gliding assay. Drag

force causes a resistance on the movement of the microtubule, slowing down its movement.

Understanding microtubule movement due to drag force allows us to understand the rate at

which microtubules pop off of kinesin motor proteins due to this, and understanding kinesin

detachment rates could result in a stronger fundamental understanding of why illnesses

related to microtubules occur. This information could help develop a more realistic model

that demonstrates how illnesses such as deafness or ALS occur [14].

2.4.   Software

From start to finish of this study, many different software had to be used to obtain the

samples and analyze them. To obtain videos of the experiments performed under the inverted

microscope, a software known as Fiji with a plug-in known as ImageJ was used. ImageJ

collects stacks of images, that when compiled and played back, acts as a video tracking the

movements of microtubules across the viewing plane. This stack of images was then

uploaded to another software, FIESTA, for further analysis.

Fluorescent Image Evaluation Software for Tracking and Analysis (FIESTA) is a

software developed in matlab that detects independent molecules or filaments within the

stack of images collected from ImageJ. FIESTA is a freeware that can be downloaded at the link: https://www.bcube-dresden.de/fiesta/wiki/FIESTA. In this research, the filament capabilities were exclusively used. FIESTA allows for simple tracking of filaments across a surface and creates paths for each clearly visible filament on the video. FIESTA tracks with nanometer precision and is fully automated to track with the input of only a few parameters (intensity, max velocity, minimum length of frames, max angle, and adjusting threshold). When this automated tracking is completed, a matlab file is exported with all the track data included. FIESTA can perform further analysis such as path statistics (plotting Gaussian curves) or even mean-square-calculations).

Matlab is the next software used in the analysis process. Matlab is a coding language that is primarily used to deal with/analyze large arrays of data. Some of its uses are math and computation, modeling, simulation, exploration, and algorithm development. As mentioned before, FIESTA is written in matlab, but for this portion of the analysis, matlab is being used independently of FIESTA. The matlab software consists of five main parts. The first is the matlab language which has control of statements, functions, data structures, and object-oriented programming. The matlab working environment is the second function which has a set of tools that work for the user. This includes the workspace and the ability to input and export data. Matlab also has the ability to handle graphics which allows for data to be analyzed and put into charts and graphs. The function library has a wide variety of algorithms that allow for functions such as sun, sine, cosine, and matrix inverse to be done. The final capability that it has is Matlab API (application program interface), which allows the user to write C and Fortran programs that interact with Matlab [1]. Many of these features have been used in this study.

Another software that was used is known as ImageJ. ImageJ is an image processing program that can display, edit, analyze, process, save and print 8 bits, 16-bit ad 32 bit images. It can support stack images, which is what the files are exported from recording the flow from the inverted microscope. It can measure distances, angles based on user defined selections and can create density histograms and line profile plots. ImageJ can also input basic shapes such as circles, ellipses, squares, or straight lines onto images. It is another freeware that can be downloaded through the link: https://imagej.nih.gov/ij/download.html. Specifically, in this work, ImageJ was used for image capture during experimentation, and analyzing exported graphs from matlab.

The final software used in this process is known as comsol, which is a Multiphysics simulation software environment. Comsol works to make simulations as realistic and accurate as possible by minimizing the assumptions the user must make. Comsol can effectively simulate electrical, mechanical, fluid, and chemical environments and within each it contains modules which are most specific to the state being simulated. For instance, for a fluid environment the user can pick from the microfluidics module, subsurface flow module, heat transfer module, etc. [11]. In this study, comsol was used specifically to simulate fluid models.

3. Methods

3.1.   Resources

3.1.1.   Gliding Assay Test

A gliding assay experiment was performed under an inverted microscope attached to a windows computer to obtain the stack of images that are worked with throughout this study. This assay test uses kinesin 1 from Drosophila melanogaster. The first step of this experiment is to prepare the kinesin being placed on the microfluidic cell and to grow the microtubules by placing it in a warm water bath. Next the chemical solution being run through the microfluidic cell is created. When all three of these are set up, they are passed into a 1 mL syringe and pushed into the microfluidic via tubing and an automated pump. First, a chemical solution is passed through, then the kinesin is passed through and attach onto the surface of the microfluidic. Next, the microtubules are passed through and attach onto the kinesin, and flow is passed over top of the kinesin and microtubule systems. The flow is passed through sequentially at various flow rates, with pauses in between the changed flow rates to capture how the microtubules behaved.

3.1.2.   Comsol

Comsol was used within this study to simulate the fluid flow throughout the flow cell. It was assumed that the plane that drag force is going to be impacting the microtubules is about 100 nanometers into the flow cell from the surface. This simulation was run for volume flow rates of 125, 250, 500, 1000, 2000, 4000, 8000, 16000, and 32000 nanoliters per second. The results of these simulations are exported as a matlab file of the velocity profiles. This matlab files

contains a V and Z file for each flow velocity simulated for instance, the 8,000

nanoliters per second would result in an array of values for V8000 and Z8000.

The array for V values represents the x data, and the array for Z values represents

the Y data. These Z and V arrays are what are plotted against each other in matlab

in order to determine the equation of best fit.

3.1.3.   FIESTA

When the videos are exported from the software and inverted microscope, it was

uploaded into FIESTA and the pixel size is set to 105. FIESTA uploads the stack of

images from the microscope and is able to play through each image as a video. All

the stacks uploaded to FIESTA had 12,000 images to complete the video. Each

image contains many specimens that are needed to be tracked. In order to identify

the objects to be analyzed, the entire stack is binarized, which essentially transfers

the picture to black and white. Binarizing converts the grayscale images into pixel

values of either 1(white) or 0(black). White occurs when the intensity of the image

is higher than a user defined intensity, and this can be seen in the grayscale

conversion below, with the white microtubules appearing whiter in the binerization

while the surrounding gray that is below the threshold appears black. This gives a

clearer identification of exactly which objects need to be tracked.
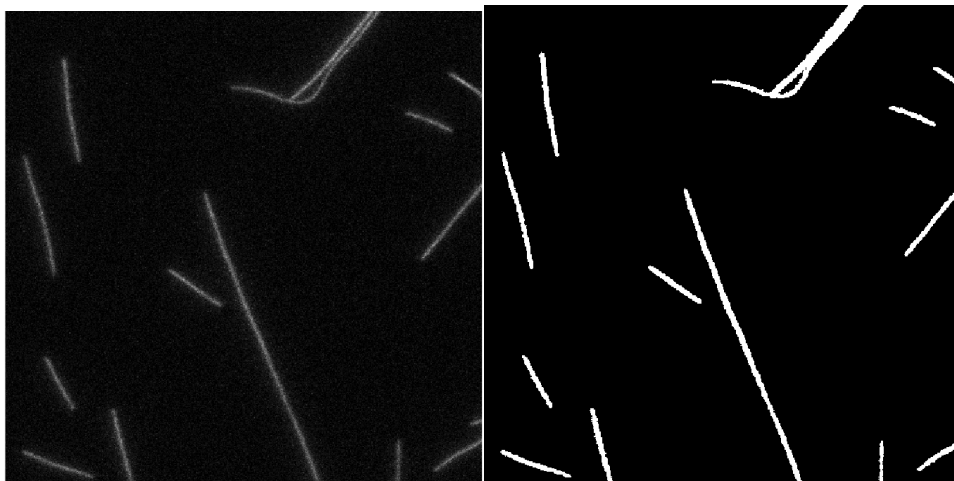
Figure 3.1 and 3.2: Stack images from microscope original and bianarized

After changing the threshold, the configuration of the stack is set up. In this

section, the settings are changed to ensure the tracking of the microtubules are as

correct and accurate as it can be. The general options are checked to ensure the pixel

size is set to a correct 105, the first frame is set to 1, and the last frame is set to

1200. In the threshold portion, the relative intensity option is selected to account for

the photo bleaching that occurred when the binary and threshold was set. Within the

tracking options, only the filament options are selected and altered. This is because

the tracking of the microtubules as whole filaments as opposed to individual

molecules is what is concerning this study.

Within the filament portion, the max velocity is set to 2,000. This is because a

typical microtubule moves at a speed of 800 nm/sec. This speed is doubled and

rounded up to account for potential outliers and catches random movement such as

fluid force. The minimum length of tracks is set to 10, if it is anything less than that,

that means the microtubules are moving too fast or coming off the kinesin too

quickly to be caught by video. The angle is also set to 359 to ensure that any strange

movements or angular changes of the microtubules are detected in the analysis. It is

not set to 360 because that value is too close to 0, and the tracked behaviors act

strangely when this setting is applied. The rest of the settings are applied, the stack

is applied to the local queue and this queue is then analyzed for tracks.

From this analysis, a set of tracks showing all the movements of the microtubules

is created. These paths are then further studied to ensure the analysis of the stacks

created reliable and consistent paths. Post tracking, the established tracks may not

be completely attached or follow along a correct path, as shown in the image of a

track below.
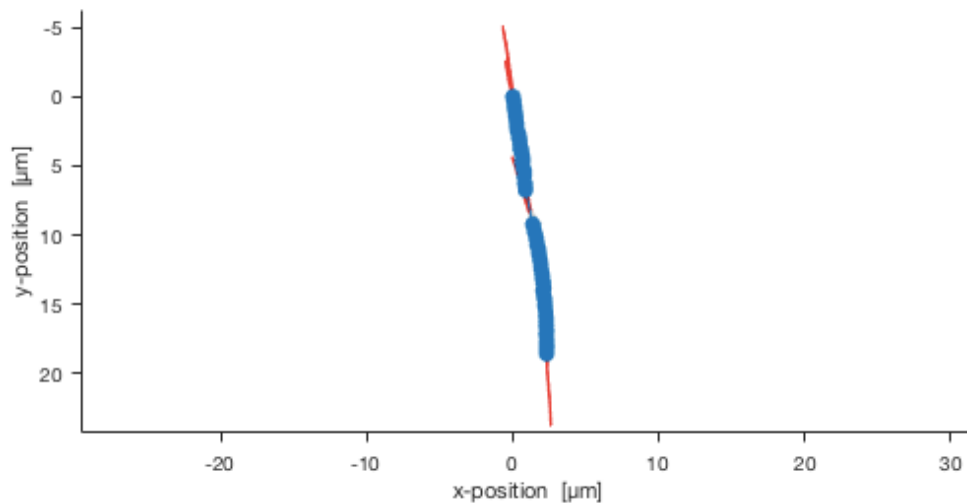
Figure 3.3: Broken microtubule track in FIESTA

That separation in the two blue segments could cause inaccuracies in measuring

velocity or force and this causes potential outliers when the data analysis is

performed in matlab. To correct these track errors, FIESTA has capabilities that

"fills in the blanks" between the different segments. To do this, the last two points

between the separation were selected, and the "track missing frames" button was

selected. Once this was done, a path was created that may or may not be directly

along the expected path. If this occurs, points were selected individually and deleted

to create a more streamlined path. When all the tracks were sorted through to ensure

smooth paths were created, they were saved as a matlab file. This was the file that

was used for further analysis

3.1.4. Matlab

Matlab was used throughout this process for analysis of data. The first time it was

used was to import the data from the comsol simulation in order to fit an equation to

the data. This was done by using the curve fitter function on matlab, and inputting a

custom equation to fit the curve to. This is shown below:
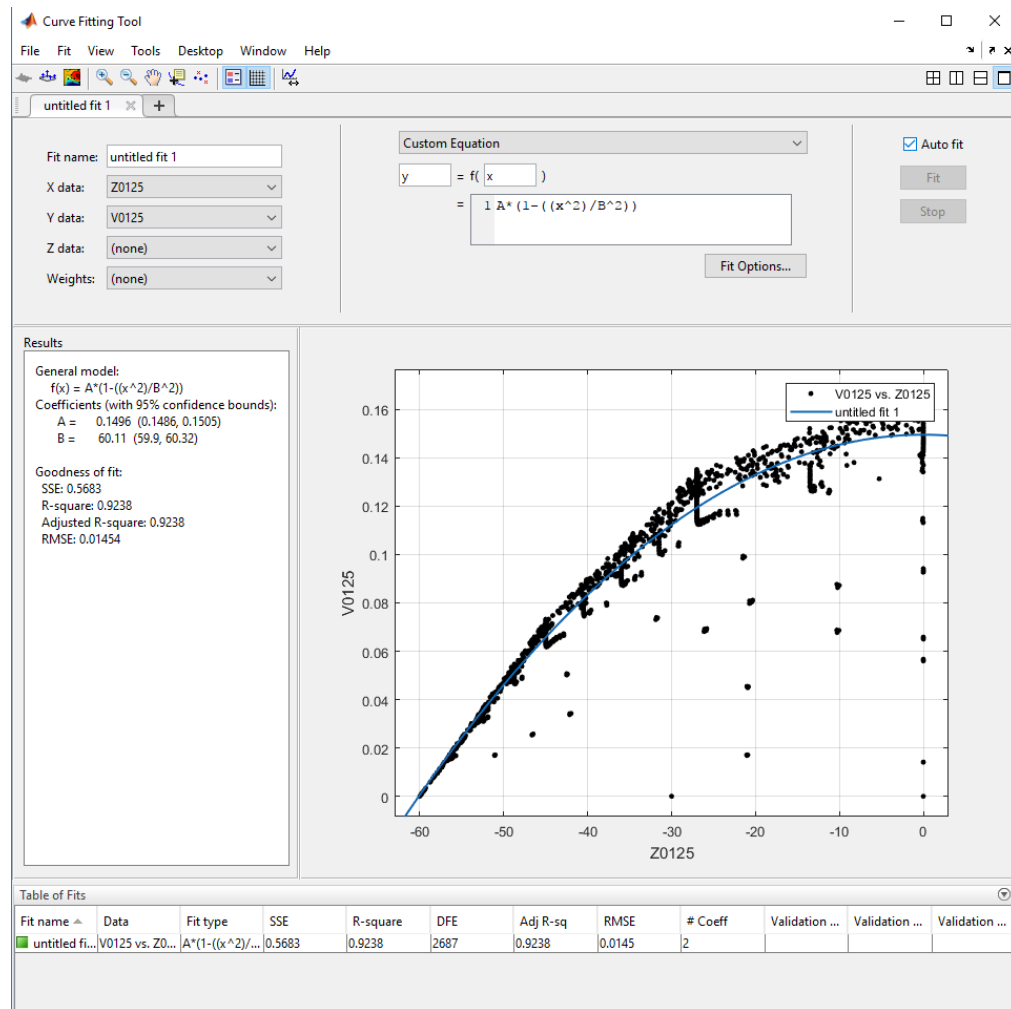
Figure 3.4: Matlab equation fitter option, fit to comsol data

The custom equation being created in this equation fitter is:

$$y = b\left(1 - \frac{x^2}{r^2}\right) \qquad \Longleftrightarrow \qquad y = V_{max}\left(1 - \frac{59.9^2}{60.11^2}\right) \qquad (3.1)$$

From this curve fitter, the constants are obtained, and the value for velocity at 59.9 microns from

the center of the fluid flow is obtained using the new equation and the constants. 59.9 microns is

used because it is where the microtubules are located relative to the z plane of the midline of the

flow cell. This is seen by the image below:

Z= 59.9 microns

Z= 0 microns

Max Velocity

Z= 59.9 microns

Figure 3.5: Side view of microfluidic channel

To obtain the velocity for flow rates that were not specifically simulated in comsol

(20,000 microns/sec), interpolation is performed. The results from this is shown in the

table below:

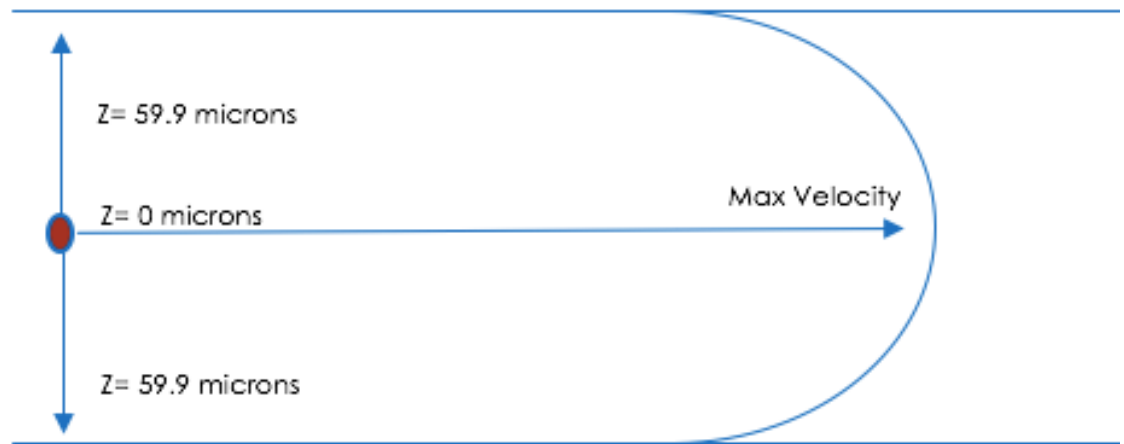| Volume Flow rate	Equation	Converted X to microns	Velocity at 59.9 microns
125	V(x) = 0.1496(1-(x^2)/(60.11 ^)2)	V(x) = 1496.(1-(x^2)/(60.11 ^)2)	0.547029
250	V(x) = .2991(1-(x^2)/(60.11 ^)2)	V(x) = 299.1(1-(x^2)/(60.11 ^)2)	1.09369
500	V(x) = .5983(1-(x^2)/(60.11 ^)2)	V(x) = 598.3(1-(x^2)/(60.11 ^)2)	2.15484
1000	V(x) =1.197(1-(x^2)/(60.11 ^)2)	V(x) =1197.0(1-(x^2)/(60.11 ^)2)	4.37696
2000	V(x) =2.393(1-(x^2)/(60.11 ^)2)	V(x) =2393.0(1-(x^2)/(60.11 ^)2)	8.75026
4000	V(x) =4.786(1-(x^2)/(60.11 ^)2)	V(x) =4786.0(1-(x^2)/(60.11 ^)2)	17.5005
8000	V(x) =9.572(1-(x^2)/(60.11 ^)2)	V(x) =9572.0(1-(x^2)/(60.11 ^)2)	35.0011
16000	V(x) =19.14(1-(x^2)/(60.11 ^)2)	V(x) =19140.0(1-(x^2)/(60.11 ^)2)	69.9875
32000	V(x) =38.29(1-(x^2)/(60.11 ^)2)	V(x) =38290.0(1-(x^2)/(60.11 ^)2)	140.012
Interpolating			
Volume Flow rate			Velocity at 59.9 microns
20000			87.4936

Table 1: Equations obtained from equation fitting and resulting velocity at 59.9 microns

These velocities were then put into a script on matlab to create a plot of theoretical perpendicular and parallel forces vs all the velocities obtained from the comsol model equations at 59.9 microns. All of the obtained velocities are put into an array. This script then begins by calculating the drag force for parallel and perpendicular microtubule movement. The difference between these two drag coefficients is that the parallel drag coefficient is 2 times that of the perpendicular, as shown below:

$$C_{D-Parallel} = \frac{(2 * \pi * \eta)}{\ln\left(\frac{2 * h}{r}\right)} \quad (3.2) \qquad C_{D-Perpendicular} = \frac{(4 * \pi * \eta)}{\ln\left(\frac{2 * h}{r}\right)} \quad (3.3)$$

In these equations, η is the viscosity of water, h is the height of the microtubule (set at 100 nm), and r is the radius of the microtubule (set at 12.5 nm because the diameter is known to be 25 nm). After this, a for loop is used to find the theoretical force values. The for loop runs from 1 to the size of the velocity element. For each one of these components, length is established as 100 nanometers (10^{-6}), and

velocity units are also changed from nanometers to meters by multiplying each

element in the array by 10^-6. Each one of these values are used in parallel and

perpendicular force calculations. A graph is then created of velocity vs parallel and

perpendicular forces for a theoretical 1 micron microtubule.

    Matlab was next used to pull specific data out of the stack pulled from FIESTA.

When the matlab file is taken from FIESTA, it contains a filament item and a

molecule item. Because only the filament tab was focused on when tracking

microtubules in FIESTA, that is the only tab that was focused on. Within the

filament item there are different categories that contain measurements pulled from

FIESTA. These categories are organized in matlab as 10 columns including: Frame

number, time, x coordinate, y coordinate, z coordinate, distance, length, amplitude,

orientation, and tag. Matlab code is broken up into numerous scripts that serve

different functions. The first three scripts written focus on calculating the drag force

and plotting that force versus the length for the three predefined volume flow rates

(8,000, 16,000, 20,000). In the first portion of this code, the drag coefficient for

perpendicular and parallel movement was calculated. When these are calculated,

they are used in further calculations for parallel force and perpendicular force

applied on the microtubule from the flow. This is done by a for loop which pulls out

the filament file from the uploaded matlab data from FIESTA. The size of the

second element of the filament is called on and the for loop runs through every

component of the second element of the filament and the results of filament are

assigned to a value "vals". "Vals" is the element that contains all 10 categories of

the element, and is what is called when all the lengths are pulled out and assigned to

a variable. When all the lengths are in one array, a distribution function is called ("fitdist") which fits a probability distribution object to the data. The "Normal" specification is called which creates a normal distribution object by fitting it to the data. The fitdist function results in an output of mu, known as the mean of the normal distribution, and sigma, known as the standard deviation. This code calls mu from the length distribution and sets it to an array of average lengths. This array is then used to calculate perpendicular and parallel force, with the equations shown below.

$$F_{parallel} = C_{D-parallel} * L_{avg} * V_{60\ micron} \qquad (3.4)$$

$$F_{perpendicular} = C_{D-paerpendicular} * L_{avg} * V_{60\ micron} \qquad (3.5)$$

Where L_{avg} is the average length obtained from the normal distribution, C_D is the drag coefficient and $V_{60\ micron}$ is the velocity obtained from the comsol model, as explained above. When parallel force, perpendicular force, and length are all found, they are plotted in two plots: Parallel Force vs Length and Perpendicular Force vs Length. Three of these script files were created, all with velocities corresponding to the flow rate being used (8,000, 16,000, and 20,000).

A function was the next script written in matlab. The function written was used to determine average angle and average velocity within a particular filament. The function inputs include the parallel and perpendicular drag coefficients, the max velocity found from the comsol model for each flow rate, and the filament. The output of the function is parallel force, perpendicular force, average velocity, and average angle. The function begins with a for loop that goes through the size of the filament component. The results of filament are assigned to a value "vals" and from

"vals", certain elements are pulled and initialized to variables. The variables initialized from filament in this function include x coordinate, y coordinate, time, and the lengths. Similar to previous scripts discussed, then a normal distribution is assigned to the lengths, and mu is called to assign it to an average label. This average length value is used in the calculation of parallel and perpendicular forces. These are then output from the function. Next, the average angle is calculated by determining new x and y values. The new x values are determined by subtracting each x value in the array from the first x value in the array. The new y value is done in a similar manner, except that entire value is then subtracted from the viewing window. The viewing window is found by multiplying the pixels/nanometer of the stack (105) by the nanometer size of the plane (512). When multiplied, a value of 53760 pixels is obtained, and by subtracting each new y value from this, the y axis is equalized to start at 0 as opposed to 53760. The lengths of the x and y paths were also found by subtracting the final position of the y or x coordinate by the first position of the y or x coordinate. These values are then used to calculate average angle using the atan2d function. This function returns an output only from -180 to 180, which is why the output value is then added to 360 within a for loop. This value is then outputted. Next, the average velocity is found within a for loop that counts from 1 to one less than the size of the x-coordinate array. Each value in the x, y and time array is subtracted from the value before it and put in an array. The velocity array is then created by performing this calculation using the difference arrays calculated prior:

$$velocity = \sqrt{\frac{(x^2 + y^2)}{t}} \qquad (3.6)$$

From this, a normal distribution is performed and the average value of this is initialized and set as an output. This function was then used in further scripts to obtain necessary outputs.

The next script written organized all the obtained angles and velocities from the output of the script into parallel and perpendicular graphs. This is done by creating a for loop with a series of nested if loops within it, to categorize each element of the average angle and average velocity elements as parallel or perpendicular. This is done with the help of a counter for both the parallel and perpendicular indexing. For each time, a value is added to the perpendicular or parallel array, the counter increases by one, so the next element added to the array is in the next spot in the array. If the first average angle pulled from the array is less than 45 °, the average angle and average velocity in the same position of the array is assigned to a new perpendicular angle and perpendicular velocity array. The index for perpendicular is also increased by 1. This same process occurs for the perpendicular array if it is greater than 135 ° and less than or equal to 225 ° or if it is greater than 315 °. This process is also the same for the parallel angles when the angle is greater than 45 ° and less than or equal to 135 ° or when the angle is greater than 225 ° and less than or equal to 315 °. When the four arrays are finally sorted (parallel velocity, parallel angle, perpendicular velocity, perpendicular angle), they are put into two scatter plots (parallel force vs parallel velocity and perpendicular force vs perpendicular

velocity). This script was created for all three selected flow velocities, utilizing all the max velocities obtained by the comsol simulation.

The final script written in matlab was used to track the path of each microtubule within each flow velocity. This is done by calling on the filament from the input matlab file from FIESTA, and assigning all the results to "vals". The third column of "vals" was then initialized to the x-coordinate array, and the fourth column of "vals" was initialized to the y coordinates. Next, similar to the function file previously talked about, the y axis is recalculated to start at zero as opposed to 53760. This is done by multiplying the multiplying the pixels/nanometer of the stack (105) by the nanometer size of the plane (512) to obtain the 53760. Next, each x coordinate is subtracted from the first coordinate in the x array to obtain a new x coordinate array. The same process is done for the y coordinate but that value is also subtracted from the value of the viewing plane (53760). The new x and y arrays are plotted against each other, but paused after each track to ensure each individual track is observed. This is done for all three flow velocities as done previously. All of these scripts are attached to the appendix of this document for further reference.

3.1.5. ImageJ

ImageJ was used during one of the final portions of the analysis. When the tracks of each microtubule were pulled from matlab, ImageJ was used to determine the radius of curvature. This was done by screenshotting the track, uploading it to ImageJ, and fitting a circle along the path of the microtubule. Then, a straight line was drawn from opposite points of the circle, creating a diameter. This line was analyzed in ImageJ to obtain a length, and was then divided by two to obtain the radius of curvature.

3.2. Design

3.2.1. Microfluidic

This experiment was performed entirely in a microfluidic environment. Microfluidics is a multidisciplinary field with applications to designing systems that work with very low volumes of fluids. Microfluidics are most commonly used in biotechnology and bioengineering because within these fields, the scale being discussed is within the nanometers or microns. The device being used in our experimentation is a microfluidic cell composed of two microscope slides attached on top of each other with a diamond sized space in the center. This diamond sized space is where the flow will be passed through, and where the kinesin and microtubule will be moving across. An example diagram and a picture are shown below:
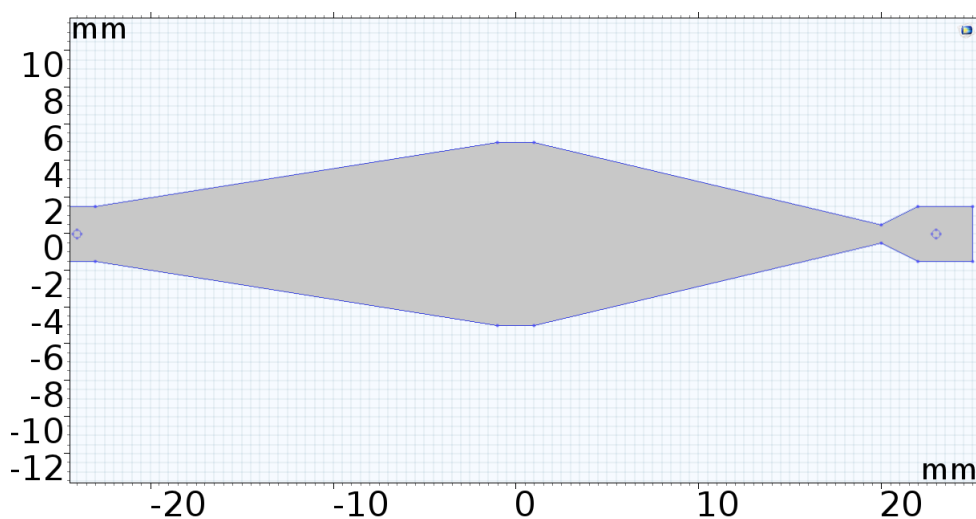

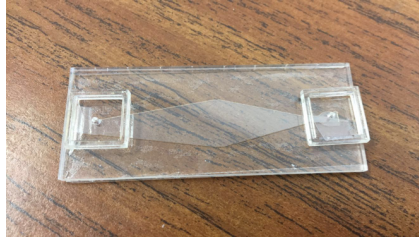*Figure 3.5: Model of microfluidic cell being used in experimentation*

Figure 3.6: Actual microfluidic cell used in experimentation

Prior to my onboarding to the project, previous microfluidic channels had been created and experimented with. Some of these prototypes included a different shaped cell (e.g. teardrop shaped) or different methods of attaching the input and output tubes. This microfluidic channel is modeled as an incompressible Newtonian fluid moving between two fixed parallel plates (two microscope slides). Because of this, it was easily defined that the flow profile within the device is laminar.

3.2.2.   Flow

The flow rate for this experiment was controlled by an automated pump and was incrementally increased. The volume flow rate began at 125 and was then increased sequentially to 250, 500, 1000, 2000, 4000, 8000, 16000, and 32000 nanoliters per second while the viewing window is still being recorded. The viewing window, as calculated before, is 53760 pixels and the portion of the microfluidic channel being recorded is where the cell area is widest, and the velocity profile is fully developed and laminar. In fluid dynamics, flow can be broken up as either laminar or turbulent flow. Laminar flow occurs typically at low velocities when fluid flow in parallel layers with no interaction or mixing between the layers. This vastly contrasts with turbulent flow, typically occurring

at higher velocities where the parallel layers interrupt each other to create eddies and swirls. The two types of flow can be seen in the image below:
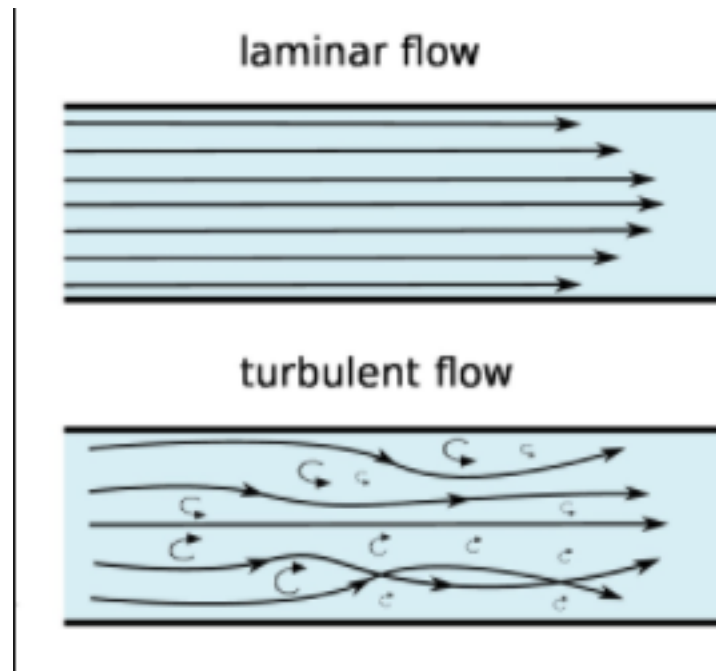
Figure 3.7: Difference between laminar and turbulent flow in two parallel cells [19]

In this experiment, it is important to keep flow laminar because this means that flow in the device will be parallel to the plates when passed through the microfluidic cell. Knowing fluid direction is critical in order to obtain the angle of interaction between the fluid flow and the microtubules and kinesin. Notice that under the laminar flow image, velocity is the fastest in the center of the viewing plane, which is the ideal situation for this experimental set up. This is because what is being researched is the effect of the full fluid force from the velocity being pushed into the microfluidic cell and this full effect is felt at the highest point in the laminar profile [4].

Another factor that is important for the flow within a microfluidic cell is to have a fully developed flow. A fully developed flow occurs when the boundary

layer (the layer between the moving fluid molecules and the stationary fluid molecules) extends to the midline of the microfluidic channel. When a fluid first enters a channel, it changes shape and may not be fully developed. It typically takes a certain length (called entrance region flow) to form a fully developed flow [21]. An image of a non-developed to fully developed flow is shown below:
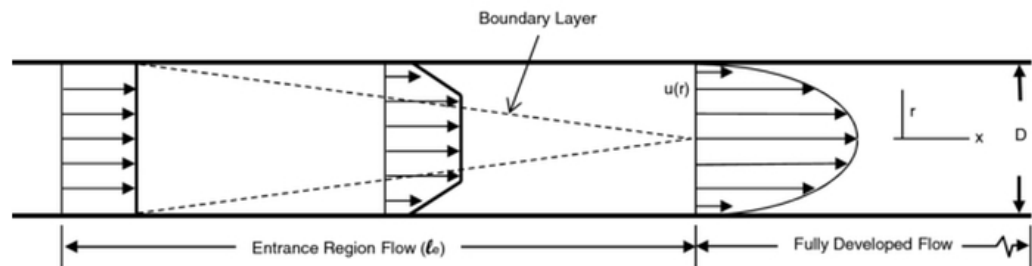
Figure 3.8: Flow within a pipe moving from non-fully developed to fully developed flow [18]

Having a fully developed flow is critical for this research because flow is laminar when it is fully developed. As seen by the image above, the flow is not a parabolic curve until it is fully developed and thus, not laminar until it is fully developed. A fully developed flow within the viewing plane is important because if there is not a constant flow or any sort of turbulence, there may be varying forces acting on the microtubules that are not accounted for by this model. This could result in swayed microtubule movements and error in the results.

4. Results and Discussion

4.1. Theoretical Results

The first step in the analysis was to determine how to compare the results we receive to a baseline. The theoretical results were the first graph obtained, which contained information for the theoretical parallel and perpendicular force vs the velocity of a 1 micron microtubule. The results for the theoretical graph is obtained from the results of the comsol simulation and the equation fitting app in matlab. This is critical in the analysis because it allows all other data to be compared to it, to understand if it is within limits or if something out of the ordinary is occurring. It can be seen that the perpendicular force (in red) is two times that of the parallel force (blue). This is expected since the equation for perpendicular force is two times that of the parallel force. It is seen that as the flow velocity increases, the parallel and perpendicular force being put on the kinesin and microtubules increases linearly. At a velocity of 125 microns/second, the velocity of a 59.9 micron microtubule is calculated to be .547029 microns/second, while for a velocity of 32000 the velocity at 59.9 microns was calculated to be 140.012 microns / second. It is these velocity values that are used in the parallel and perpendicular force calculations which result in the range of velocity being from 0-150 microns per second and the range of forces to be from 0-.8 Newtons.
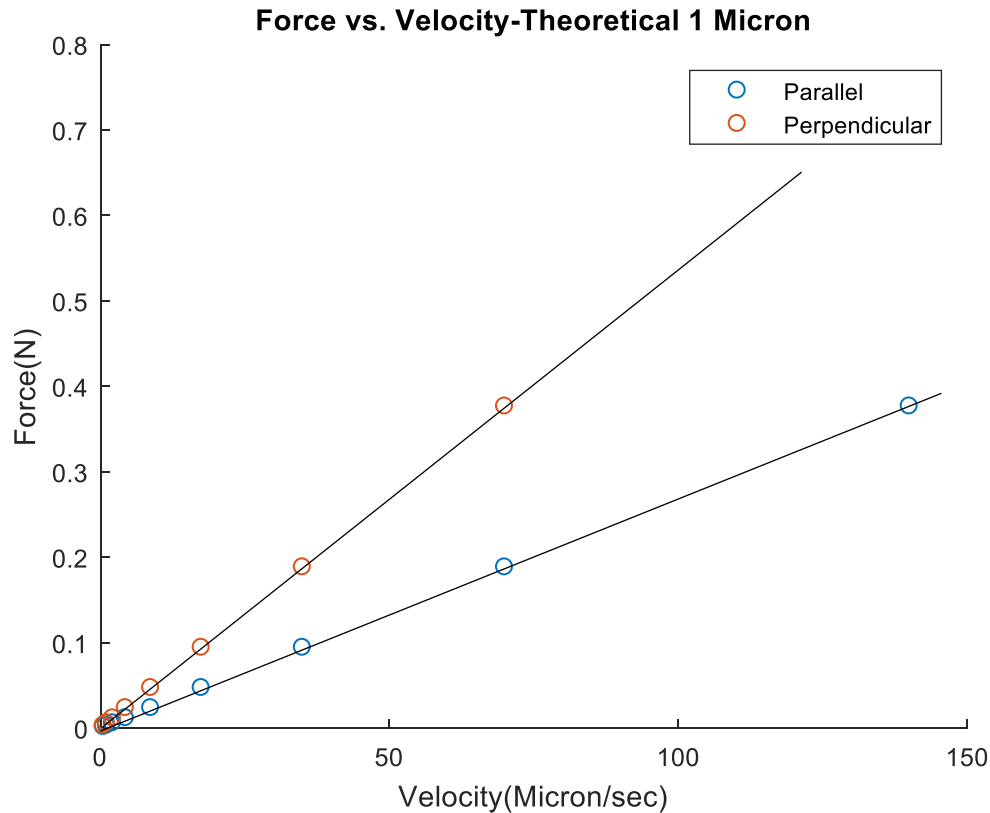
Figure 4.1: Theoretical force vs microtubule velocity showing perpendicular and parallel force. This data was calculated based on flow simulations done in comsol simulation of the fluid flow in a chamber. The data pulled from the comsol simulation was then graphed in matlab and analyzed with an equation fitter in figure 3.4 to obtain the various points seen plotted. The blue points are for parallel microtubule position and the red points are for perpendicular microtubule position which were calculated using equations 3.1-3.5.

Once the theoretical graph was created, the remainder of the data from the various

volume flow rates could be analyzed and compared to this baseline. The first two factors

addressed was the force vs length, because length is one of the greatest determining

factors of drag force, as show in equation 3.4 and 3.5.

4.2.   Force vs. Length Plots

The next plot that was focused on was the force vs. length plots. The question

posed here was: how does the length of the microtubule affect the amount of drag force

being applied to it, and what are the trends in this relationship? How could we use this

information to determine force sensitivity of the microtubules? For each flow rate used in this analysis, two force vs length plots were created (parallel force vs. Length and perpendicular force vs length). The plots for the 8,000 nanoliters/second flow rate is shown below. It is seen that there is an increase of a factor of 2 between the perpendicular and parallel forces. For example, the highest parallel force on the graph below is 3 pN while for the perpendicular force, it is double that at 6 pN. This makes sense mathematically because the equation for perpendicular drag force (eqn. 3.3) is multiplied by a factor of 2 compared to the equation for parallel drag force (eqn. 3.2). This makes sense conceptually because a microtubule that is moving parallel to the flow velocity will have less surface area available for the fluid force to be pushing against, as opposed to a microtubule that is moving perpendicular to the flow and has its entire length exposed to the fluid flow. Another trend that is identified is that as microtubule length increases, so does both the perpendicular and parallel drag force it takes to stall the microtubule. This makes sense because the equation for parallel and perpendicular force are dependent on velocity, drag coefficient, and length. Because the force is directly dependent on length, the longer the microtubule is, the more drag force is applied to is. The longer the microtubule is, the more surface area is exposed to the fluid and can feel the effects of the flow moving past it.

Force vs Length for a Volume Flow Rate of 8000 nL/sec

Figure 4.2: Parallel and Perpendicular Force vs microtubule length under a volume flow rate of 8000 nL/sec. Data for this was obtained through a gliding assay experiment using kinesin-1 and microtubules while a sequentially increased flow was passed over them. The film was tracked in FIESTA for paths of each microtubule at the specified flow rate. The filament files from FIESTA were then analyzed in MATLAB to calculate flow using equations 3.2 to 3.6 and the variables from the filament file such as x, y, z coordinates, length, and max velocity obtained from the previous Comsol model.

From the graphs above, it is clear that at length of 35 microns, the parallel and perpendicular force are going to be much stronger than a microtubule at a length of 5 microns. Another way the importance of length is seen in this experiment is seen from the layout of the data points. Because the experiment and flow run over the microtubules was done sequentially, it can be seen that only the longer microtubules last at the highest flow velocities. The force vs length graphs for other flow velocities are shown below in figures 4.3 and 4.4.
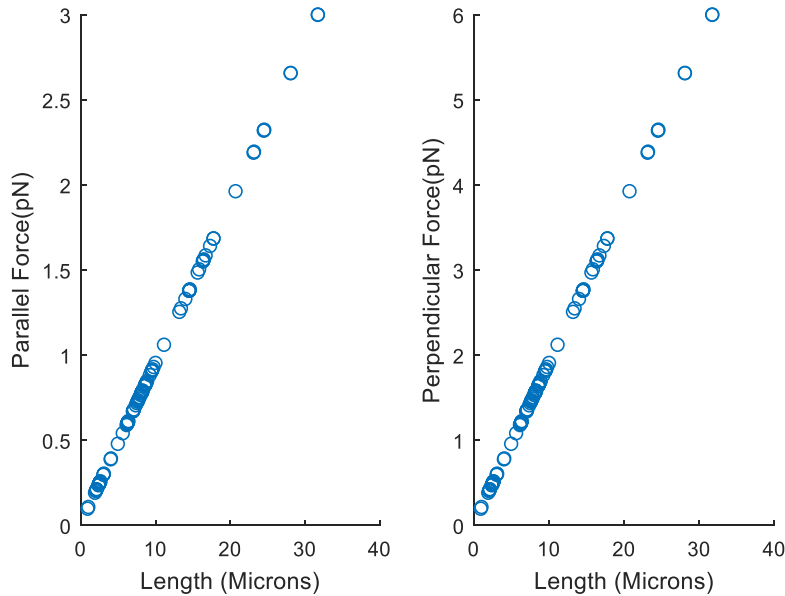
Figure 4.3: *Parallel and Perpendicular Force vs microtubule velocity under a volume flow rate of 16000 nL/sec. Data for this was obtained through a gliding assay experiment using kinesin-1 and microtubules while a sequentially increased flow was passed over them. This is the second speed the volume flow rate was increased to from 8000 nL/sec. The film was tracked in FIESTA for paths of each microtubule at the specified flow rate. The filament files from FIESTA were then analyzed in MATLAB to calculate flow using equations 3.2 to 3.6 and the variables from the filament file such as x, y, z coordinates, length, and max velocity obtained from the previous Comsol model.*
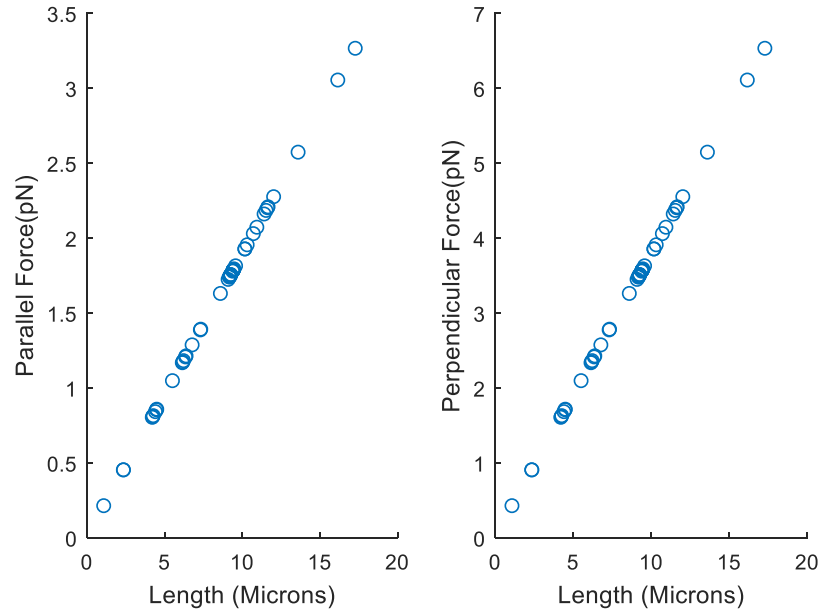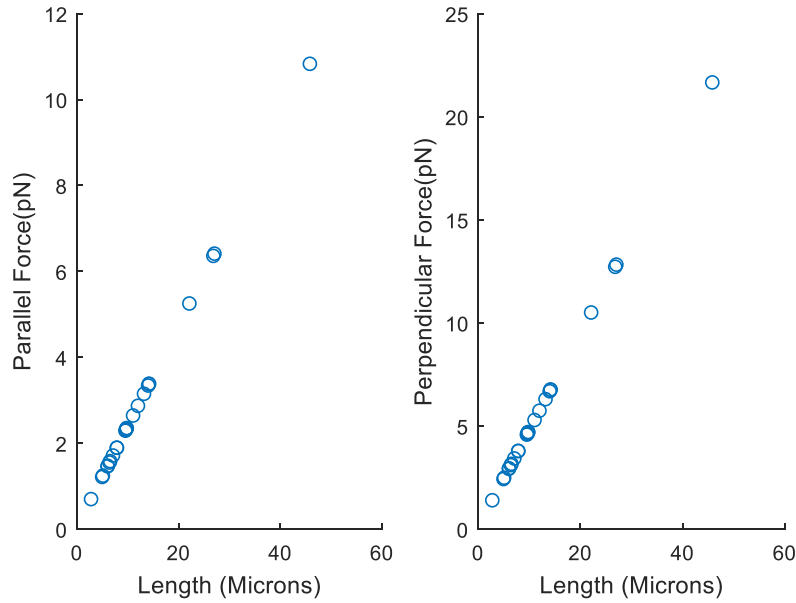
Figure 4.4: Parallel and Perpendicular Force vs microtubule velocity under a volume flow rate of 20000 nL/sec. Data for this was obtained through a gliding assay experiment using kinesin-1 and microtubules while a sequentially increased flow was passed over them. This is the third speed the volume flow rate was increased to from 16000 nL/sec. The film was tracked in FIESTA for paths of each microtubule at the specified flow rate. The filament files from FIESTA were then analyzed in MATLAB to calculate flow using equations 3.2 to 3.6 and the variables from the filament file such as x, y, z coordinates, length, and max velocity obtained from the previous Comsol model.

In all of these figures, there is a linear relationship between length and force, and as length of the microtubule increases, so does the drag force it is experiencing along it. This is the same for both parallel and perpendicular drag force. It is important to note that in the graphs for a volume flow rate of 20,000 nL/second, there is an outlier at the length of 50 microns that was not present in previous graphs. This value appeared based on tracking error in FIESTA where a track was incorrectly measured. This value is an outlier from the length distribution and can be neglected.

4.3.   Angle vs Average Velocity Plots

The next portion of the analysis focused on angles vs average velocity. It is understood that orientation is critical for the amount of drag force that the microtubules experience.

Based on previously known relationships of inclination and drag as well as the relationship between surface area and drag (double the area, double the drag) it was expected that as volume flow rate increases, perpendicularly oriented microtubules will stall and then pop off, leaving mostly parallel alignments of microtubules. This is because perpendicularly oriented microtubules have more surface area exposed to the flow of the fluid as opposed to parallel orientation. This is shown below:
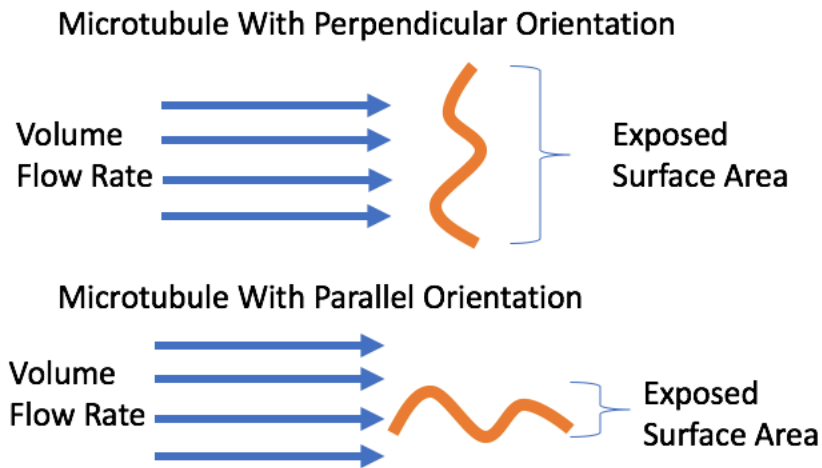
Figure 4.5: Diagram demonstrating the relationship between microtubule orientation and exposed surface area to the flow moving past it

This relationship is also shown through the Bernoulli equation:

$$R = \frac{1}{2}\rho C A v^2 \qquad (4.1)$$

where R is drag force, ρ is density, C is drag coefficient A is surface area and v is speed. This means it is also expected that with higher surface area exposure (perpendicular angles) the velocity should slow down due to increased drag force [6]. The question posed was, can this be confirmed through our obtained data? After angles are calculated in matlab, they are sorted to parallel and perpendicular arrays, they are plotted versus velocity to identify any

trends or correlations. Three plots were created, one for each volumetric flow rate. These

plots are shown below:

Figure 4.6: Average Angle vs Microtubule Velocity at three different volume flow rates (a) flow rate of 8000 nL/sec (b) flow rate of 16000 nL/sec (c)flow rate of 20000 nL/sec using kinesin 1 within a gliding assay. The perpendicular and parallel angles were sorted for all the microtubules oriented at all three volume flow rates. On each graph, perpendicular and parallel microtubule orientation are shown as well as the associated degree and velocity. The angles for orientation were binarily decided and the cut off was 45 degrees in the negative and positive direction from the x axis on both sides of the y axis. If it fell between this cutoff, it was classified as perpendicular, and anything outside of this cutoff was classified as parallel.

The graphs include both perpendicular and parallel angles and associated velocities. As

seen on the graph, there is a clear distinction between when the angle is parallel

(45<angle≤135, or 225<angle≤315) and when it is perpendicular (135<angle≤225 or

315<angle). The sequential nature of this experiment is also shown again, as there are

many more points on the graph of 8,000 nL/sec than there are on the graph of 20,000

nL/sec because many of the microtubules have popped off at this point due to fluid force.

Of the microtubules that last through to the highest flow rate, most of them move in the

parallel direction. This data is understandable since it is harder for a flow to remain

perpendicular when a fluid force is pushing it in the parallel direction due to the

previously stated relationship of surface area and drag.

4.4. Force vs Average Velocity Plots

The next two factors that were analyzed was the relationship between force and

velocity to understand how drag force is affected by the volume flow rate being passed

over it, and how the velocity of the microtubules change in accordance with that. This

was done to confirm the expected relationship that drag force increases with increased

volume flow rate, which is shown in equation 4.1. The next graphs that were created were

drag force vs average velocity plots. These plots were created for all three flow rates used

in this experiment. The force vs velocity graphs show the drag force caused from the

volume flow rate. These plots organize data to show that as the flow rate increases, due to

the sequential nature of this experiment, many of the points drop off. Again, this is

caused by microtubules losing the connection to kinesin and popping off, leaving only the

strongest connected microtubules at the highest flow rate. These plots show that the

perpendicular oriented microtubules have the most drag force applied to them.

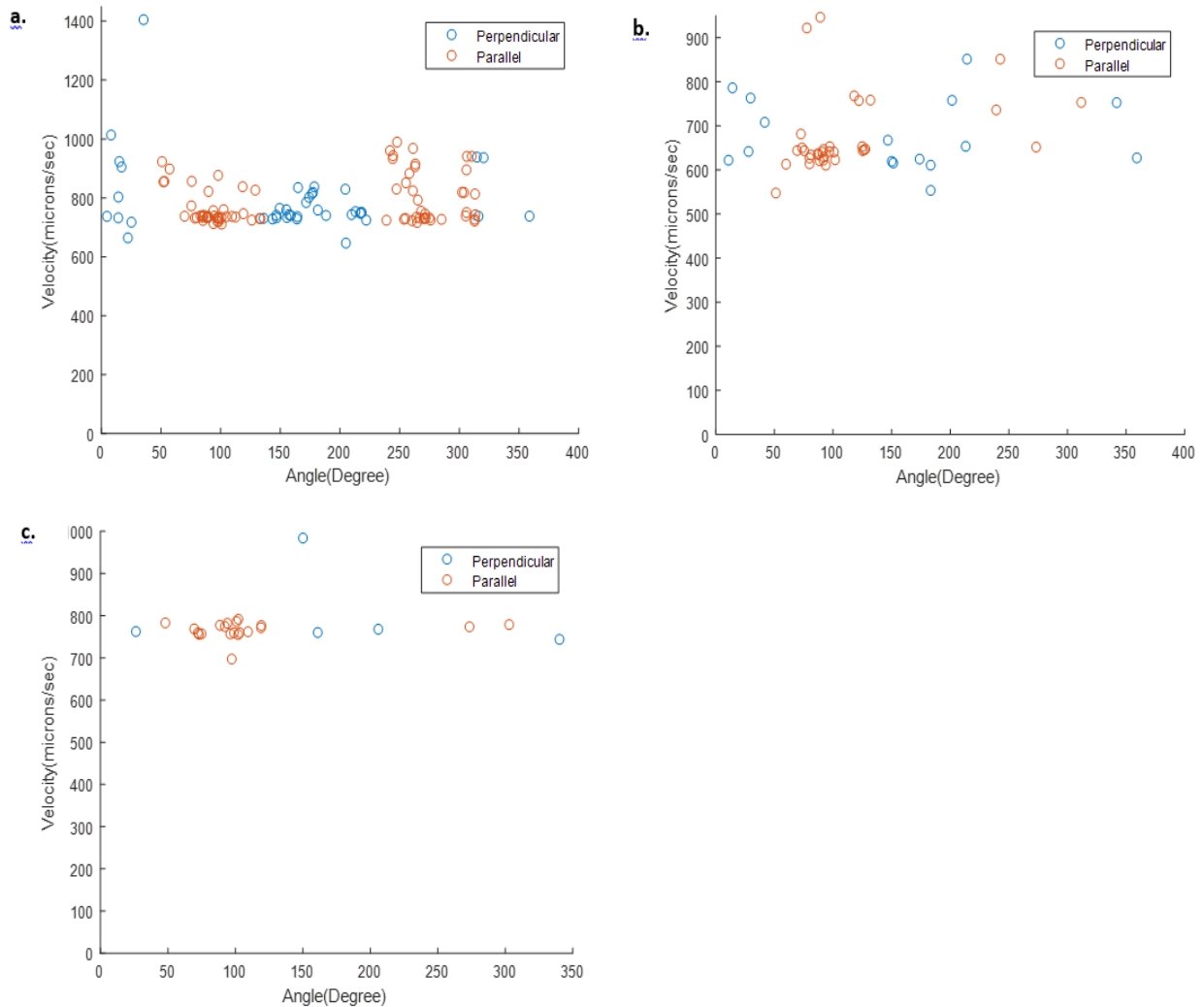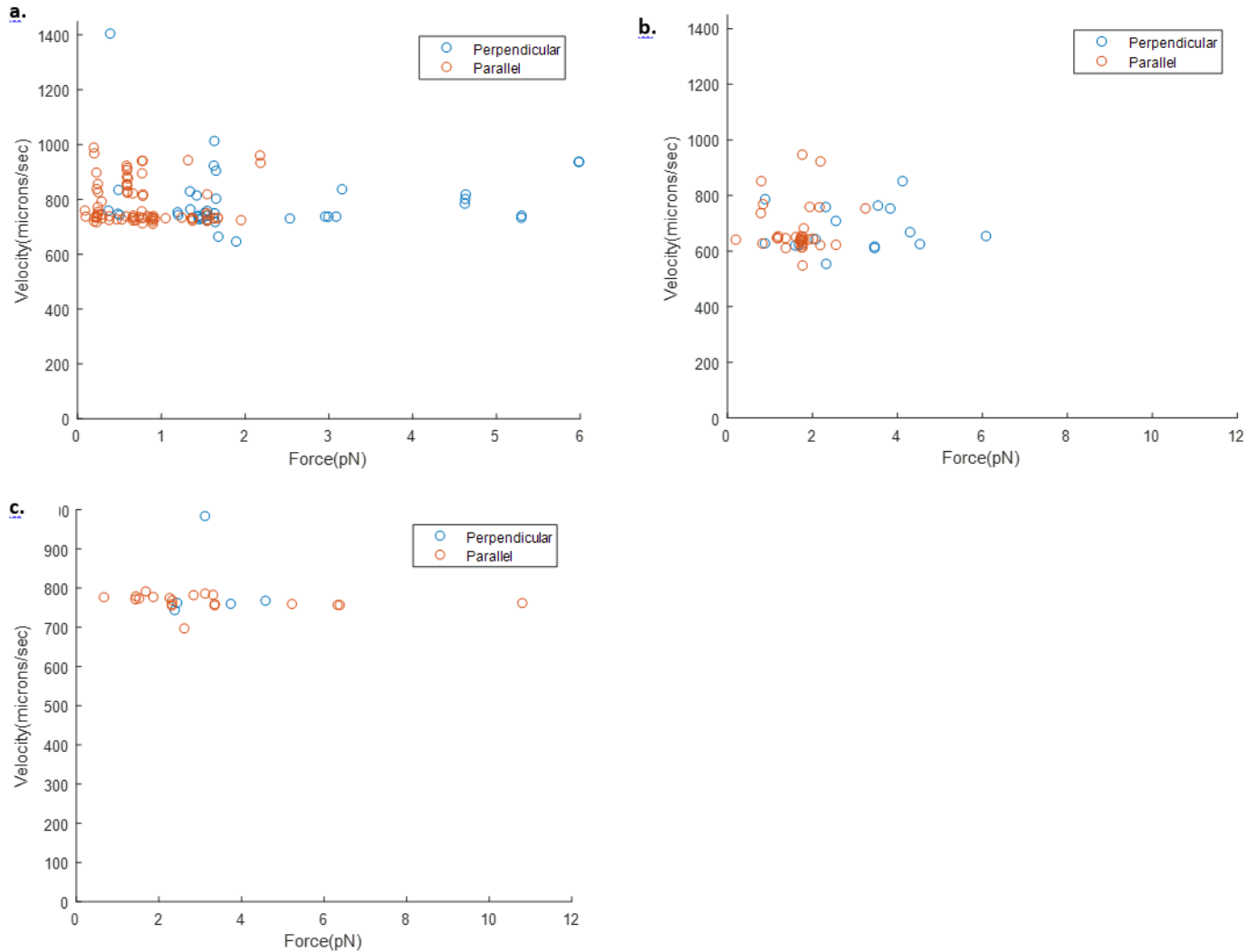*Figure 4.7: Average Angle vs Drag Force at three different volume flow rates (a) flow rate of 8000 nL/sec (b) flow rate of 16000 nL/sec (c)flow rate of 20000 nl/sec using kinesin 1 within a gliding assay. The perpendicular and parallel angles were sorted for all the microtubules oriented at all three volume flow rates. On each graph, perpendicular and parallel microtubule orientation are shown as well as the associated force and velocity. The angles for orientation were binarily decided and the cut off was 45 degrees in the negative and positive direction from the x axis on both sides of the y axis. If it fell between this cutoff, it was classified as perpendicular, and anything outside of this cutoff was classified as parallel.*

At the highest flow rate, there are only four perpendicular oriented microtubules left. This

means that at some point between a flow rate of 16,000 and 20,000 nL/sec, a majority of the

perpendicular oriented microtubules had enough fluid force applied to them to pop off the

popped off. In the flow rate of 20,000 nL/sec, there is again an outlier at a force of 12 pN that

came from previous data pulled from FIESTA. Another pattern that can be identified from these graphs is that the typical velocity that a microtubule moves is between 600-1000 microns/sec. This range gets smaller as the flow velocity increases, so for a flow rate of 20,000 nL/sec the range is between 650-850 microns/sec.

4.5.   Summary Plots

Once the force vs velocity was plotted on a scatter plot, further analysis was performed to delve deeper into the potential trends or relationships that arise between these two factors. This was done through bean plots. The first two bean plots that were created were the parallel and perpendicular forces applied from each volume flow rate compared to each other. As seen below, there is a much larger and clumped together set of data for the flow rate of 8,000 nL/sec than for the flow rate of 20,000 nL/sec. There are also many less points, and an outlier due to the earlier error in length distribution is present again in the 20,000 flow rate. There are also many more points for the parallel plot than the perpendicular plot, again due to the amount of force that is pushed against the microtubule and causes them to reorient themselves in a parallel direction.
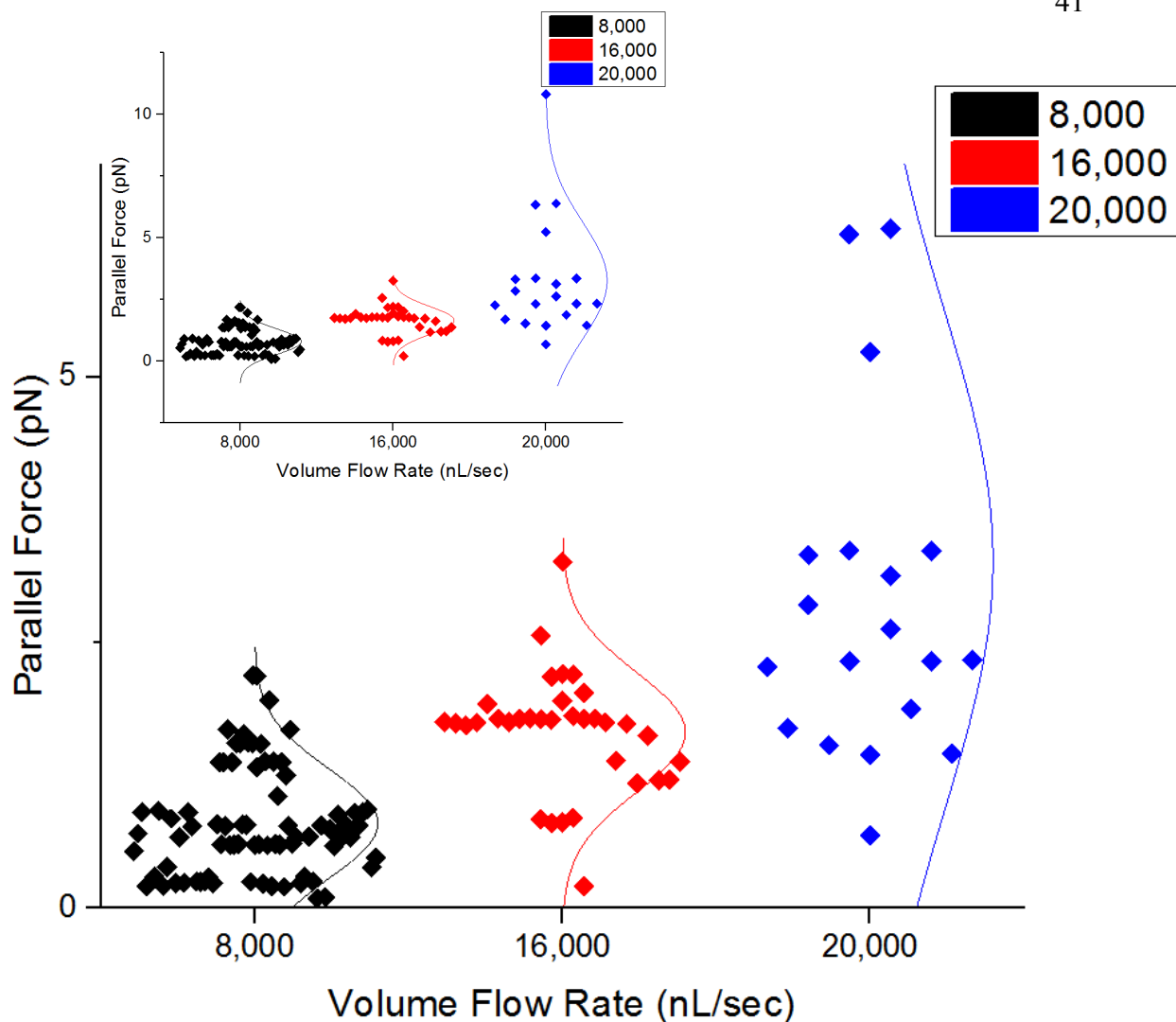
Figure 4.8: Summary Plot for parallel force for each volume flow rate passed over the microtubules within the gliding assay. This was performed using Kinesin 1 with sequential increases of volume flow rates. Based on the length distribution obtained from FIESTA, at a volume flow rate of 20,000 nL/sec, an outlier was obtained, and is shown in the upper left-hand corner of the figure.
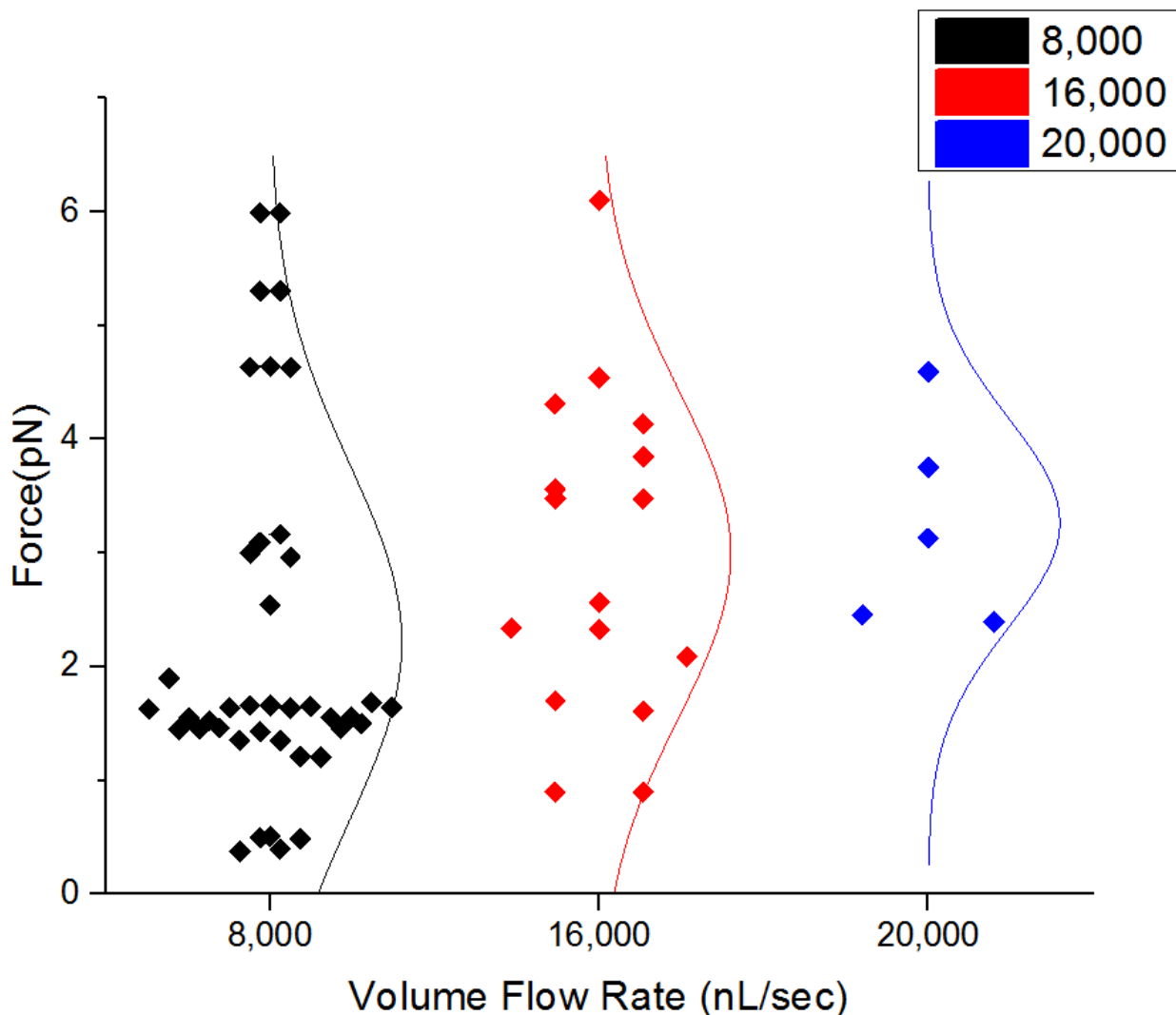
Figure 4.9: Bean Plot for perpendicular force for each volume flow rate passed over the microtubules within the gliding assay. This was performed using Kinesin 1 with sequential increases of volume flow rates.

The next graphs that were created were general force vs velocity graphs with 3 different Bins (.5, 1, 2). The difference between these plots and previous plots is that force was not split between perpendicular and parallel, they were all grouped together with their associated velocities. These graphs were created in excel and were used to understand the relationship between force and cooperativity of kinesin. From the graphs below, it can be seen that there is no identified relationship between the amount of drag force experienced on a microtubule,

and the velocity of the microtubule moving. As the force increases, the only factor that changes are the amount of data points present. This value decreases with increasing force because the drag force overpowers the attachment force of the kinesin to the microtubules, thus they pop off. Despite the fact that the data is being affected by the amount of force being applied, there is still no clear stall rate present or any identifiable "tipping point" for when the drag force overpowers. The microtubule velocity remains well within expected range between 600-900 microns/sec even with increased drag force.
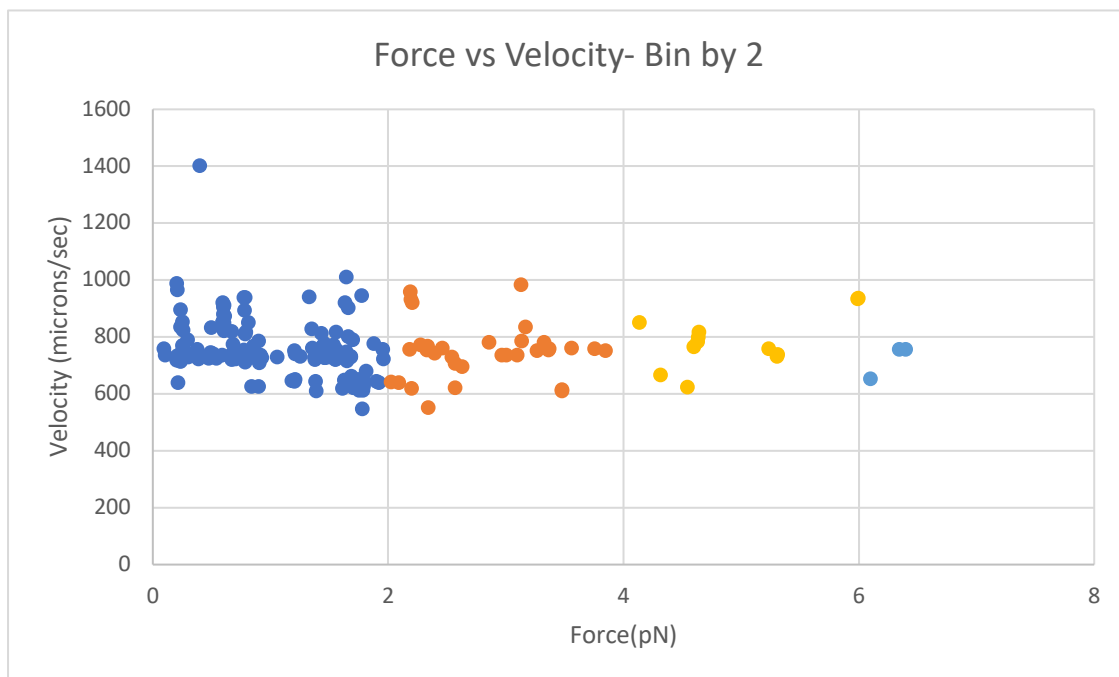
Figure 4.10: Plot for force vs velocity at all the volume flow rates with a Bin of 2

Figure 4.11: Plot for force vs velocity at all the volume flow rates with Bin of 1
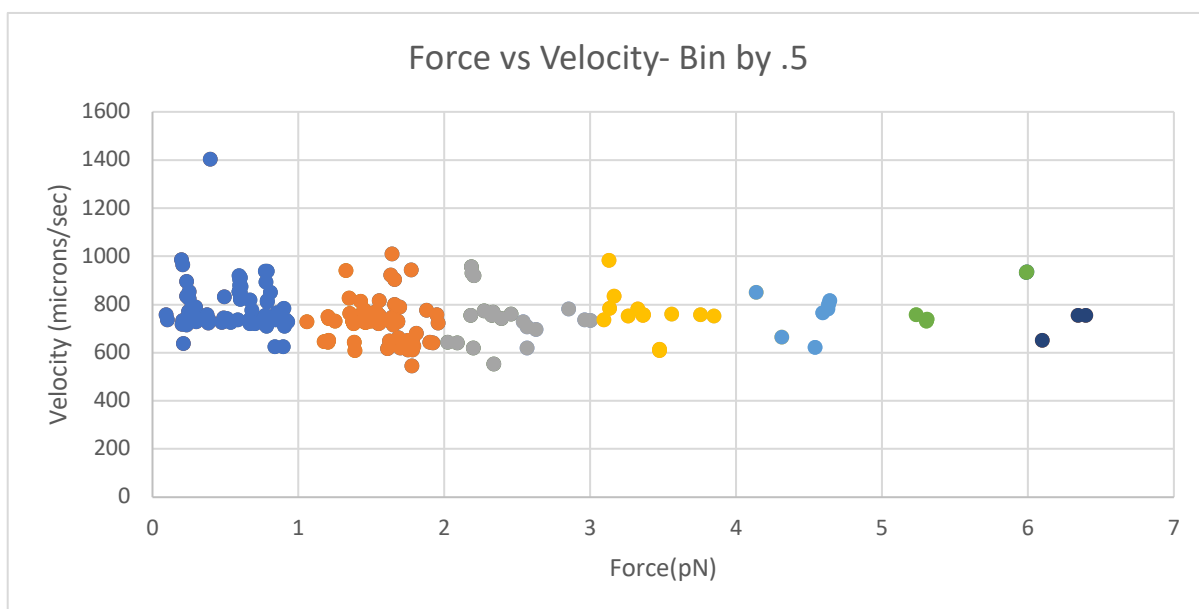
Figure 4.12: Plot for force vs velocity at all the volume flow rates with Bin of .5

5. Conclusion
5.1.　　Specimen Results

Based on the experiments performed and the analysis done, a conclusion is reached that the drag forces caused by the fluid flow is working independent of cooperativity. The relationship between force and cooperativity has not reached a threshold or "tipping point" where it is yet identifiable that the rela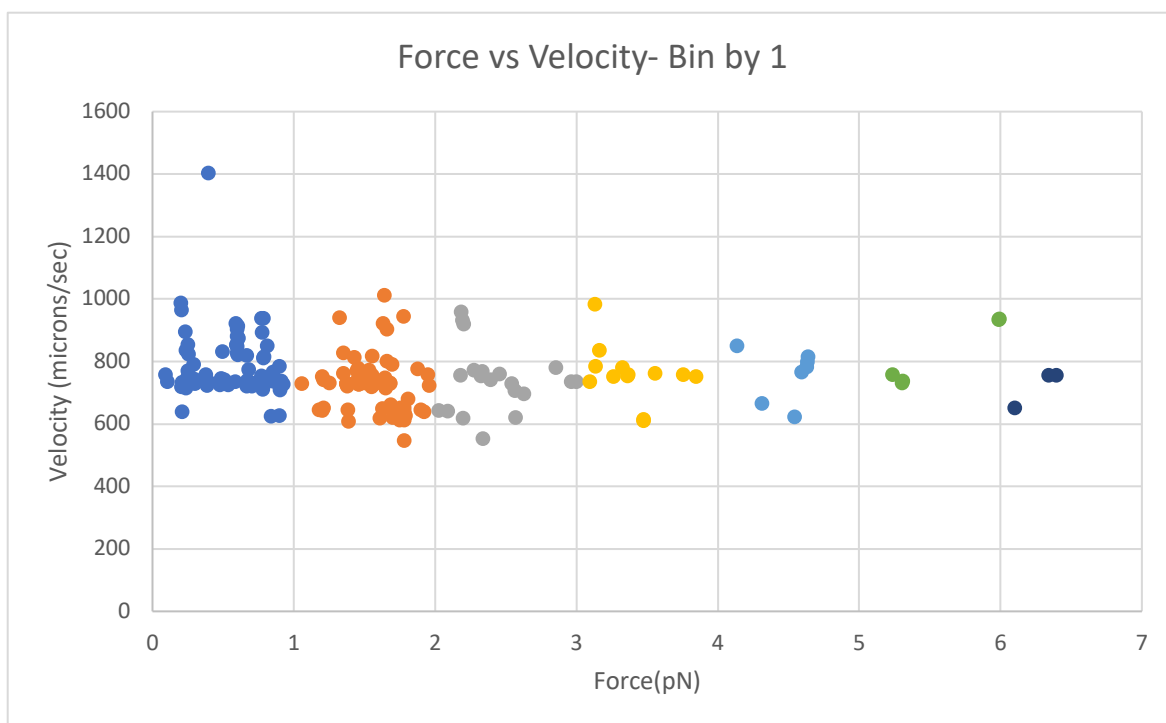tionship between each kinesin is cooperative and they are working together or if they are independent of each other. Based on the results showing that the kinesin still remained attached to the microtubule despite increasing drag force, a few conclusions and resolutions can be made. The first is that the kinesin being is used is too strong, thus the kinesin is not overpowered by the drag force, and the microtubule remains on the surface, not demonstrating any detachment as desired. The kinesin used, kinesin 1, has demonstrated cooperative behavior in the past and that is why it is being used in this experiment but it may also have a strong binding strength that must be taken account for. A resolution to this would be to use a more force sensitive kinesin such as kinesin 2 or 3. Next, it could be concluded that the flow used was not strong enough. If the kinesin does have a strong binding characteristic, the volume flow rates that were used to create a drag force was not strong enough and in order to break those strong bonds between the microtubule and kinesin, the drag force must be increased. This can be done by functionalizing the microtubule. This means that a linker (optical bead) is placed on the end of the microtubule which increases the surface area of the microtubule, creating more of a drag force. This bead also provides a point source where both the drag force and force of the microtubule moving are acting directly against everything in the network. It provides a point of detachment that is easily identifiable, so it is clear what the interaction between kinesin detachments are. This means that if the bead detaches, and the entire microtubule detaches, the motors are working

independently of each other and it is stochastic. On the contrary, if the bead detaches and the remainder of the microtubule is attached, cooperativity is examined. Finally, another conclusion that could be drawn is that there may have been too many kinesin placed on the surface of the microfluidic, which meant for each microtubule, an excess of binding and support was present to keep it attached to the kinesin. A resolution to this would be to perform this same experiment but pass a lower concentration kinesin solution through the microfluidic so each microtubule is not saturated with kinesin.

5.2.   Future Work

The results of this study have set the groundwork to move forward with future research. The purpose of this research is to establish a screening method to understand if a microtubule is stochastic or cooperative in order to understand the behavior of the microtubule. This experiment and analysis confirmed that there is no relationship between the drag force and the cooperativity of the kinesin, as discussed previously. The future work for this study would include to delve deeper into the conclusions drawn by testing the resolutions presented. The next step would be run a similar analysis on data pulled from an experiment which either increased drag force, decreased kinesin concentration, or used a more force sensitive kinesin. The best approach that would serve our function for understanding motor cooperativity would be to increase the drag force by attaching an optical bead. This not only increases drag force but also serves as an easy identifier for when the threshold for cooperativity is reached, which is the purpose of this study.

Another path that could be taken to move forward is to break up the FIESTA film data into contour lengths. Contour length is the length of the microtubule at longest possible extension. For each contour length, a force diagram can be created, and then it is easy to

identify the amount of force per kinesin from that microtubule. These graphs demonstrate force sensitivity, and based on sensitivity, a screening process can be pulled to determine if the kinesin is stochastic or cooperative.

References

[1] Ackerman, S. *What is Matlab*,

from http://cimss.ssec.wisc.edu/wxwise/class/aos340/spr00/whatismatlab.htm

[2] Block, S. M. Optical tweezers: a new tool for biophysics. *Noninvasive Techniques in Cell Biology*.

[3] Childs, G. (2014). *Cilia, flagella, and centrioles*, from http://cytochemistry.net/cell-biology/cilia.htm

[4] Davis, W. *Microfluidics and Fluid Dynamics*, from http://beweb.ucsd.edu/courses/senior-design/projects/2015-2016/Website_Group_13/microfluidics-and-fluid-dynamics.html

[5] Duke, T. (2000). Cooperativity of myosin molecules through strain–dependent chemistry: The Royal Society.

[6] Elert, G. (1998-2018). *Aerodynamic Drag*. The Physics Hypertextbook.

[7] Endow , S., Kull , F. J., & Liu, H. (2010). Kinesin at a Glance. Journal of Cell Science.

[8] Fazal, F., & Block, S. (2012). Optical tweezers study life under tension. *Net Photonics*.

[9] Furuta, K. y., Furuta, A., Toyoshima , Y., Amino , M., Oiwa , K., & Kojima , H. (2013). Measuring collective transport by defined numbers of processive and nonprocessive kinesin motors. *PNAS*.

[10]   Gough, J., Karplus, K., Hughey, R., & Chothia, C. (2001). Assignment of Homology to Genome Sequences using a Library of Hidden Markov Models that Represent all Proteins of Known Structure. Journal of Molecular Biology.

[11]   Griesmer, A. (2013). *What is COMSOL Multiphysics?*,

from https://www.comsol.com/blogs/what-is-comsol-multiphysics/

[12]   Hall, N. (2015). *What is Drag?*, from https://www.grc.nasa.gov/www/k-
12/airplane/drag1.html

[13]   Hao , L., & Scholey, J. (2009). Intraflagellar transport at a glance (pp. 889-892). Journal
of Cell Science: The Company of Biologist.

[14]   Hayashi, K., Pack, C., Sato, M., Mouri, K., Kaizu, K., Takahashi, K., et al. (2013).
Viscosity and drag force involved in organelle transport: investigation of the fluctuation
dissipation theorem. The European Physical Journal E.

[15]   Hendricks, A., Epureanu, B., & Meyhöfer , E. (2009). *Cooperativity of multiple kinesin-
1 motors mechanically coupled through a shared load*,
from https://www.sciencedirect.com/science/article/pii/S0167278909000037

[16]   Howard, J., Vallee, R. B., Bloom, G. S., Pereira, A., & Goldstein, L. S. B.
(1996). *Kinesin-1*, from https://labs.cellbio.duke.edu/kinesin/Kinesin.html

[17]   Inoue, Y., Toyoshima, Y. Y., Iwane, A. H., Morimoto, S., Higuchi, H., & Yanagida, T.
(1997). Movements of truncated kinesin fragments with a short or an artificial flexible neck
(Vol. 94, pp. 7275–7280). Biophysics.

[18]   Jamison, D., Driver, J., & Diehl, M. (2012). Cooperative responses of multiple kinesins
to variable and constant loads. *The Journal of Biological Chemistry*.

[19]   *Laminar vs. Turbulent Flow*. from https://www.cfdsupport.com/OpenFOAM-Training-
by-CFD-Support/node275.html

[20]   Mandelkow, E., & Mandelkow , E.-M. Kinesin motors and disease. *Cell Biology*.

[21]   Molki, A., Khezzar, L., & Goharzdeh, A. (2013). *Measurement of fluid velocity
development in laminar pipe flow using laser Doppler velocimetry*,
from http://iopscience.iop.org/article/10.1088/0143-0807/34/5/1127

[22]   *Muscular System: Stages of A Muscle Contraction*.

from http://legacy.owensboro.kctcs.edu/gcaplan/anat/notes/api%20notes%20j%20%20muscle%20contraction.htm

[23]   Prevo, B., Mangeol, P., Oswald, F., Scholey, J., & Peterman, E. (2015). Functional differentiation of cooperating kinesin-2 motors orchestrates cargo import and transport in *C. elegans* cilia (pp. 1536 – 1545). *Nature Cell Biology*.

[24]   Rai, A., Rai, A., Ramaiya, A., Jha, R., & Mallik, R. (2013). Molecular adaptations allow dynein to generate large collective forces inside cells. *Cell*.

[25]   Rajagopal, I. (2008). *Cytoskeleton 2*, from http://oregonstate.edu/instruction/bi314/summer08/cytotwo.html

[26]   Rosenbaum, J., & Witman, G. (2002). Intraflagellar Transport (pp. 813 – 825). *Nature Reviews Molecular Cell Biology*.

[27]   Ruhnow, F., Zwicker, D., & Diez, S. (2001). Tracking Single Particles and Elongated Filaments with Nanometer Precision (Vol. 100). Biophysical Journal.

[28]   Schirber, M. (2015). *Focus: Stalling a Molecular Motor*, from https://physics.aps.org/articles/v8/114

[29]   Svoboda, K., Schmidt, C. F., Schnapp, B. J., & Block, S. M. (1993). Direct observation of kinesin stepping by optical trapping interferometry. Nature.

[30]   Uppulury , K., Efremov , A., Driver, J., Jamison, D. K., Diehl , M., & Kolomeisky, A. (2013). Analysis of Cooperative Behavior in Multiple Kinesins Motor Protein Transport by Varying Structural and Chemical Properties. Cellular and Molecular Bioengineering.

[31]   Vilfan, A., Frey, E., Schwabl, F., Thormählen, M., Song, Y., & Mandelkow, E. (2001). Dynamics and cooperativity of microtubule decoration by the motor protein kinesin, *Journal of Molecular Biology* (Vol. 312, pp. 1011-1026).

[32]   Wortman, J., Shrestha, U., Barry, D., Garcia, M., Gross, S., & Yu, C. (2014). Axonal Transport: How High Microtubule Density Can Compensate for Boundary Effects in Small-Caliber Axons. Biophysics Journal.

[33]   Yildiz, A., Tomishige, M., Vale, R., & Selvin, P. (2004). Kinesin Walks Hand-Over-Hand. Science Magazine.

Appendix A

```
%Code to Plot theoretical plot of Force vs Velocity
Cdpar=(2*pi*(8.9*10^-4))/(log(200/25));
Cdperp=(4*pi*(8.9*10^-4))/(log(200/25));

Vel_100nm=[0.547029 1.09369 2.15484 4.37696 8.75026 17.5005 35.0011 69.9875
140.012] ;
for i=1:size(Vel_100nm,2)
    l=1*10^-6;
    v=Vel_100nm(i)*10^-6;
    fpar(i)=Cdpar *l*v;
    fperp(i) = Cdperp*l*v;
end
figure(1),scatter(Vel_100nm,fpar*10^12)
hold on
scatter(Vel_100nm,fperp*10^12)
title ('Force vs. Velocity-Theoretical 1 Micron')
xlabel ('Velocity(Micron/sec)')
ylabel('Force(N)')
legend('Parallel', 'Perpendicular')

%Code to plot the force vs length for a flow rate of 8000

Cdpar=(2*pi*(8.9*10^-4))/(log(200/25));
Cdperp=(4*pi*(8.9*10^-4))/(log(200/25));
vmax=35.0011;

for i=1:size(Filament,2)
    vals=Filament(i).Results;
    len=vals(:,7);
    l_dist=fitdist(len,'Normal');
    lavg(i)=l_dist.mu;
    fpar(i)=Cdpar *(lavg(i)*10^-3*vmax);
    fperp(i)=Cdperp *(lavg(i)*10^-3)*vmax;
end


figure
subplot(1,2,1)
scatter(lavg/1000, fpar)
xlabel ('Length (Microns)')
ylabel('Parallel Force(pN)')

subplot(1,2,2)
scatter(lavg/1000,fperp)
xlabel ('Length (Microns)')
ylabel('Perpendicular Force(pN)')
suptitle('Force vs Length for a Volume Flow Rate of 8000 nL/sec')




%Code to plot the force vs length for a flow rate of 16000
```

```matlab
Cdpar=(2*pi*(8.9*10^-4))/(log(200/25));
Cdperp=(4*pi*(8.9*10^-4))/(log(200/25));
vmax16000=69.9875;

for i=1:size(Filament,2)
    vals=Filament(i).Results;
    len=vals(:,7);
    l_dist=fitdist(len,'Normal');
    lavg(i)=l_dist.mu;
    fpar(i)=Cdpar *(lavg(i)*10^-3)*vmax16000;
    fperp(i)=Cdperp *(lavg(i)*10^-3)*vmax16000;
end

subplot(1,2,1)
scatter(lavg/1000, fpar)
xlabel ('Length (Microns)')
ylabel('Parallel Force(pN)')

subplot(1,2,2)
scatter(lavg/1000,fperp)
xlabel ('Length (Microns)')
ylabel('Perpendicular Force(pN)')
suptitle('Force vs Length for a Volume Flow Rate of 16000 nL/sec')

%Code to plot the force vs length for a flow rate of 20000


Cdpar=(2*pi*(8.9*10^-4))/(log(200/25));
Cdperp=(4*pi*(8.9*10^-4))/(log(200/25));
v20000=87.4936;

for i=1:size(Filament,2)
    vals=Filament(i).Results;
    len=vals(:,7);
    l_dist=fitdist(len,'Normal');
    lavg(i)=l_dist.mu;
    fpar(i)=Cdpar *(lavg(i)*10^-3)*v20000;
    fperp(i)=Cdperp *(lavg(i)*10^-3)*v20000;
end

subplot(1,2,1)
scatter(lavg/1000, fpar)
xlabel ('Length (Microns)')
ylabel('Parallel Force(pN)')

subplot(1,2,2)
scatter(lavg/1000,fperp)
xlabel ('Length (Microns)')
ylabel('Perpendicular Force(pN)')
suptitle('Force vs Length for a Volume Flow Rate of 20000 nL/sec')

% Code to plot Angle vs Velocity and Force vs Velocity for Flow rate of
% 8,000
perp_start=1;
par_start=1;
```

```
Cdpar=(2*pi*(8.9*10^-4))/(log(200/25));
Cdperp=(4*pi*(8.9*10^-4))/(log(200/25));
v8000=35.0011;

    [ fpar,fperp,avg_ang, avg_vel ] = Avg(Cdpar,Cdperp, v8000, Filament);
    for k = 1:size(avg_ang,2)
    if avg_ang(k) <= 45
        perp(perp_start)= avg_ang(k);
        perp_avg_vel(perp_start) = avg_vel(k);
        perp_force(perp_start) = fperp(k);
        perp_start= perp_start+1;
        elseif avg_ang(k)>45
            if avg_ang(k) <= 135
                par(par_start)=avg_ang(k);
                par_avg_vel(par_start) = avg_vel(k);
                par_force(par_start) = fpar(k);
                par_start= par_start+1;
            elseif avg_ang(k) > 135
                if avg_ang(k) <=225
                    perp(perp_start)= avg_ang(k);
                    perp_avg_vel(perp_start) = avg_vel(k);
                    perp_force(perp_start) = fperp(k);
                    perp_start= perp_start+1;
                elseif avg_ang(k) >225
                    if avg_ang(k) <= 315
                        par(par_start)=avg_ang(k);
                        par_avg_vel(par_start) = avg_vel(k);
                        par_force(par_start) = fpar(k);
                        par_start= par_start+1;
                    elseif avg_ang(k) > 315
                        perp(perp_start)= avg_ang(k);
                        perp_avg_vel(perp_start) = avg_vel(k);
                        perp_force(perp_start) = fperp(k);
                        perp_start= perp_start+1;
                    end
                end
            end
        end
    end
    clear vel

figure
scatter(perp_force,perp_avg_vel)
xlabel ('Force(pN)')
ylabel('Velocity(microns/sec)')
hold on
scatter(par_force,par_avg_vel)
axis([0 6 0 1450])
legend('Perpendicular', 'Parallel')

figure
scatter(perp,perp_avg_vel)
xlabel ('Angle(Degree)')
ylabel('Velocity(microns/sec)')
hold on
scatter(par, par_avg_vel)
```

```matlab
axis([0 400 0 1450])
legend('Perpendicular', 'Parallel')

% Code to plot Angle vs Velocity and Force vs Velocity for Flow rate of
% 16,000
perp_start=1;
par_start=1;
Cdpar=(2*pi*(8.9*10^-4))/(log(200/25)); %unit: pa *s
Cdperp=(4*pi*(8.9*10^-4))/(log(200/25));
vmax16000=69.9875;

    [ fpar,fperp,avg_ang, avg_vel ] = Avg(Cdpar,Cdperp, vmax16000, Filament);
    for k = 1:size(avg_ang,2)
    if avg_ang(k) <= 45
        perp(perp_start)= avg_ang(k);
        perp_avg_vel(perp_start) = avg_vel(k);
        perp_force(perp_start) = fperp(k);
        perp_start= perp_start+1;
        elseif avg_ang(k)>45
            if avg_ang(k) <= 135
                par(par_start)=avg_ang(k);
                par_avg_vel(par_start) = avg_vel(k);
                par_force(par_start) = fpar(k);
                par_start= par_start+1;
            elseif avg_ang(k) > 135
                if avg_ang(k) <=225
                    perp(perp_start)= avg_ang(k);
                    perp_avg_vel(perp_start) = avg_vel(k);
                    perp_force(perp_start) = fperp(k);
                    perp_start= perp_start+1;
                elseif avg_ang(k) >225
                    if avg_ang(k) <= 315
                        par(par_start)=avg_ang(k);
                        par_avg_vel(par_start) = avg_vel(k);
                        par_force(par_start) = fpar(k);
                        par_start= par_start+1;
                    elseif avg_ang(k) > 315
                        perp(perp_start)= avg_ang(k);
                        perp_avg_vel(perp_start) = avg_vel(k);
                        perp_force(perp_start) = fperp(k);
                        perp_start= perp_start+1;
                    end
                end
            end
        end
    end
    clear vel

figure
scatter(perp_force,perp_avg_vel)
xlabel ('Force(pN)')
ylabel('Velocity(microns/sec)')
hold on
scatter(par_force,par_avg_vel)
axis([0 12 0 1450])
legend('Perpendicular', 'Parallel')
```

```
figure
scatter(perp,perp_avg_vel)
xlabel ('Angle(Degree)')
ylabel('Velocity(microns/sec)')
hold on
scatter(par, par_avg_vel)
axis([0 400 0 950])
legend('Perpendicular', 'Parallel')

% Code to plot Angle vs Velocity and Force vs Velocity for Flow rate of
% 20,000
perp_start=1;
par_start=1;
Cdpar=(2*pi*(8.9*10^-4))/(log(200/25));
Cdperp=(4*pi*(8.9*10^-4))/(log(200/25));
v20000=87.4936;

    [ fpar,fperp,avg_ang, avg_vel ] = Avg(Cdpar,Cdperp, v20000, Filament);
    for k = 1:size(avg_ang,2)
    if avg_ang(k) <= 45
        perp(perp_start)= avg_ang(k);
        perp_avg_vel(perp_start) = avg_vel(k);
        perp_force(perp_start) = fperp(k);
        perp_start= perp_start+1;
        elseif avg_ang(k)>45
            if avg_ang(k) <= 135
                par(par_start)=avg_ang(k);
                par_avg_vel(par_start) = avg_vel(k);
                par_force(par_start) = fpar(k);
                par_start= par_start+1;
            elseif avg_ang(k) > 135
                if avg_ang(k) <=225
                    perp(perp_start)= avg_ang(k);
                    perp_avg_vel(perp_start) = avg_vel(k);
                    perp_force(perp_start) = fperp(k);
                    perp_start= perp_start+1;
                elseif avg_ang(k) >225
                    if avg_ang(k) <= 315
                        par(par_start)=avg_ang(k);
                        par_avg_vel(par_start) = avg_vel(k);
                        par_force(par_start) = fpar(k);
                        par_start= par_start+1;
                    elseif avg_ang(k) > 315
                        perp(perp_start)= avg_ang(k);
                        perp_avg_vel(perp_start) = avg_vel(k);
                        perp_force(perp_start) = fperp(k);
                        perp_start= perp_start+1;
                    end
                end
            end
        end
    end
    clear vel

figure(1)
```

```matlab
scatter(perp_force,perp_avg_vel)
xlabel ('Force(pN)')
ylabel('Velocity(microns/sec)')
hold on
scatter(par_force,par_avg_vel)
axis([0 12 0 1000])
legend('Perpendicular', 'Parallel')

figure(2)
scatter(perp,perp_avg_vel)

xlabel ('Angle(Degree)')
ylabel('Velocity(microns/sec)')
hold on
axis([0 350 0 1000])
scatter(par, par_avg_vel)
legend('Perpendicular', 'Parallel')


%function file to obtain forces and average angle and velocity
function [ fpar,fperp,avg_ang, avg_vel ] = avg(Cdpar,Cdperp, vmax, Filament )
for i=1:size(Filament,2)
    vals=Filament(i).Results;
    x=vals(:,3);
    y=vals(:,4);
    len=vals(:,7);
    l_dist=fitdist(len,'Normal');
    lavg(i)=l_dist.mu;
    fpar(i)=Cdpar  *(lavg(i)*10^-3)*vmax;
    fperp(i)=Cdperp *(lavg(i)*10^-3)*vmax;
    x_new=x-x(1);
    y_new=53760-(y-y(1));
    t= vals(:,2);
    xdiff=x_new(end)-x_new(1);
    ydiff=y_new(end)-y_new(1);
    avg_ang(i)=atan2d(ydiff,xdiff);
    if avg_ang(i)<0
        avg_ang(i)=(360+avg_ang(i));
    end

    for j=1:size(x)-1
      xdiff1=x(j+1)-x(j);
      ydiff1=y(j+1)-y(j);
      tdiff = t(j+1)-t(j);
      vel(j)= sqrt((xdiff1)^2+(ydiff1)^2)/tdiff;
    end
   f=fitdist(vel','Normal');
    avg_vel(i)=f.mu;

end
```

Appendix B

Permanent Address
Verona, NJ 07044

Campus Address
State College, PA 16802

Soufieh Hakimzadeh

Phone: (973) 979-7250 | Email: smh6112@psu.edu

EDUCATION   **Bachelor of Science in Mechanical Engineering**
Bachelor of Science in Engineering Science -Honors Curriculum
Minor in Engineering Mechanics
The Pennsylvania State University, University Park, PA

GPA: **3.37/4.00**
Anticipated Graduation: May 2018

SENIOR THESIS

Title: **Analysis of Effects of Mechanical Forces in Kinesin and Microtubules Within a Gliding Assay**

- Studied literature regarding biomechanics to establish a background when designing innovative wetlab experiments
- Partnered with PhD candidates and performed experiments to explore various mechanical effects within a constant biologic system to determine biomechanical properties such as effects of fluid force or magnetic attraction
- Analyzed data obtained from experiments using Fiesta software to identify trends or unpredictable biological patterns

WORK EXPERIENCE

Research Assistant, Hancock Lab   August 2016-Current
University Park, PA

- Collaborate with graduate students and professors to achieve research goals using a hybrid biological engineered system to study the molecular biomechanics of kinesin motor
- Investigate applications of the kinesin-microtubule systems in designed and prototyped microfluidic channels

Engineering Operations Leadership Development Program Intern, Siemens Healthcare   May 2017-August 2017
Walpole, MA

- Assisted in increasing production line productivity by making obsolete and replacing 22% of the current automations
- Communicated with cross functional teams and external vendors to ensure new machines or parts are being properly designed and manufactured for the site
- Supported validation and implementation of an automated heat sealer used to optimize pack preparation time for quality testing in laboratory diagnostics
- Investigated volumetric measuring tools used in clean space manufacturing areas, analyze results with department heads and write risk assessments regarding the possible variance in batch records

Quality Assurance Co-op, Johnson & Johnson- Janssen Biotech   January 2016-June 2016
Malvern, PA

- Implemented metrics, timelines, and tracking tools to manage Batch Records for each production stage and increase efficiency by ~ 20%
- Developed and modified Standard Operating Procedures and practices to ensure all documentation and manufacturing changes were in compliance with FDA regulations
- Lead and streamlined aspects of the release process continuous improvement initiative to ensure delivery of the highest quality documentation

Lecture Assistant, Penn State Biology Department   August 2015-December 2015
University Park, PA

- Assisted professors in delivering lecture instruction to various class sizes
- Performed administrative duties including grading papers and supporting exam preparation for students
- Allocated additional time to support students to further enhance their understanding of the class content

Research Assistant, Assis Laboratory   January 2015-May 2016
University Park, PA

- Applied computational and statistical methods to address questions in evolutionary genomics
- Researched and analyzed gene duplication and its role in evolutionary phenotypes through Perl programs

SOFTWARE   Java, Perl, SolidWorks, Microsoft Office, Adobe Illustrator, MATLAB, Visio, MTrackJ, Fiesta, Photoshop, Mathmatica, CAD, Simulink, Multisim

SKILLS   Fluent in Farsi, with a basic understanding of Spanish, Finite Element Analysis, Collaborative, Strong Technical Writing Skills

LEADERSHIP &   **Web Coordinator,** Society of Engineering Science '17-'18
INVOLVEMENT   **Member**, Society of Women Engineers (PSU) '14-'18
                      Engineering Career Envoy, College of Engineering '16-'18
                      Academic Committee, Penn State Engineering House '15
                      Moral & Fundraising Committee, Tetra Thon Org '14-'17

Campus Ambassador, WayUp '18
Staff, Campus Recreation & Facilities '17-'18
Academic Facilitator, Penn State WEP '15-'18
Founder, Penn State PAWs '16
EMR, Verona Rescue Squad '13-'17

HONORS   **Recipient**, Kerns-McNitt Engineering Science Award (Spring '17)
                      Recipient, Dean's List (Fall '15, Fall'16)
                      Recipient, Montclair Women's Club Volunteering Scholarship (Summer '14)
                      Recipient, President's Silver and Bronze award for Volunteering (Fall '14, Fall '13)
                      Recipient, Verona Rescue Squad Volunteer Award (Summer '14)
                      Honorable Mention, WEP Joelle Leadership Award (Spring '17)